



UNIVERSITA' DEGLI STUDI DI VERONA

DEPARTMENT OF NEUROSCIENCE, BIOMEDICINE AND MOVEMENT

GRADUATE SCHOOL OF LIFE AND HEALTH SCIENCES

DOCTORAL PROGRAM IN

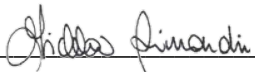
*NEUROSCIENCE, PSYCHOLOGICAL AND PSYCHIATRIC SCIENCES,
AND MOVEMENT SCIENCES*

36° / 2020

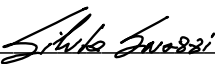
*Spatiotemporal dynamics of visuospatial orienting, reorienting and
updating processes: a behavioral and functional investigation*

S.S.D. M-PSI/01

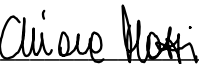
Coordinator: Prof.ssa Michela Rimondini

Signature 

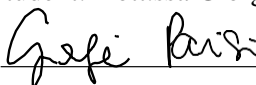
Tutor: Prof.ssa Silvia Savazzi

Signature 

Co-Tutor: Dott.ssa Chiara Mazzi

Signature 

Doctoral Student: Dott.ssa Giorgia Parisi

Signature 

This work is licensed under a Creative Commons Attribution-NonCommercial-NoDerivs 3.0 Unported License, Italy. To read a copy of the licence, visit the web page:

<http://creativecommons.org/licenses/by-nc-nd/3.0/>



Attribution — You must give appropriate credit, provide a link to the license, and indicate if changes were made. You may do so in any reasonable manner, but not in any way that suggests the licensor endorses you or your use.



NonCommercial — You may not use the material for commercial purposes.



NoDerivatives — If you remix, transform, or build upon the material, you may not distribute the modified material.

Spatiotemporal dynamics of visuospatial orienting, reorienting and updating processes: a behavioral and functional investigation - Giorgia Parisi

PhD Thesis

Verona 6 Marzo 2024

ISBN code

SOMMARIO

Negli ultimi venti anni, il mondo della ricerca neuroscientifica ha visto un incremento di lavori dedicati allo studio dell'attenzione visuospatiale, stimolato dall'idea incentrata sull'esistenza di due network cerebrali attenzionali volti, rispettivamente, allo spostamento volontario dell'attenzione e al riorientamento attenzionale verso eventi inattesi. Nonostante vi sia un discreto accordo sulle principali regioni cerebrali che costituiscono tali network (ossia un network dorsale responsabile dello spostamento attentivo "goal-directed", chiamato DAN, e un network ventrale dedicato al riorientamento dell'attenzione, chiamato VAN), alcuni aspetti necessitano ancora di essere chiariti. Questo concerne in particolare il contributo specifico di ogni regione cerebrale e la relazione tra i due network, necessaria per favorire un controllo attenzionale flessibile.

Con questo lavoro abbiamo quindi cercato di fare chiarezza su tali questioni ancora irrisolte tramite l'utilizzo di approcci comportamentali e funzionali innovativi e all'avanguardia.

Nel primo studio, per la raccolta dei dati funzionali è stata infatti impiegata una recente e promettente tecnica denominata Event-Related Optical Signal (EROS), applicata durante lo svolgimento di un compito attentivo di detezione (derivante dal noto paradigma di Posner). Lo scopo di tale studio era quello di definire le dinamiche spazio-temporali dei processi attenzionali ed esaminare le interazioni predittive sia all'interno di ogni sistema attenzionale sia tra di essi.

Le analisi funzionali, ottimizzate dall'applicazione di un'ulteriore analisi chiamata Granger Causality Analysis, hanno rivelato uno scambio predittivo e ricorrente tra determinate regioni parietali dorsali e aree visive, da cui sembrerebbe dipendere sia il processo di orientamento che di riorientamento attenzionale. Inoltre, è stato evidenziato un contributo specifico da parte del network ventrale dell'emisfero sinistro nel dirigere l'attenzione dopo la comparsa di un cue centrale e predittivo. Al contrario, l'attività studiata nel network ventrale dell'emisfero destro sembrerebbe riflettere un processo post-percettivo di aggiornamento delle aspettative interne legate al compito. Questa evidenza deriva specificatamente dallo

studio della giunzione temporoparietale di destra, una regione cerebrale che rappresenta uno dei nodi essenziali costituenti il VAN.

In linea con il primo, il secondo studio esposto in questa tesi, è stato condotto al fine di comprendere ulteriormente il ruolo di rTPJ nei processi attentivi visuospatiali. Più precisamente, mentre i partecipanti di questo studio svolgevano un compito attentivo di discriminazione (derivante dal sopracitato paradigma di Posner) abbiamo applicato in modo ripetitivo e in corrispondenza di rTPJ, la tecnica transcranial magnetic stimulation (rTMS, tre impulsi a 20 Hz, per ogni trial). Ciò ci ha consentito di interferire con l'attività di rTPJ ed osservare eventuali effetti comportamentali legati o al processo di riorientamento o al meccanismo di aggiornamento delle predizioni interne riguardanti le associazioni cue-stimolo trial dopo trial. Le analisi comportamentali hanno corroborato i risultati del nostro primo studio: rTPJ sembra essere coinvolta nell'abilità cognitiva di aggiornare i modelli interni contestualmente connessi alle contingenze del compito.

L'ultimo studio di questo lavoro, prevedeva l'esplorazione dell'implementazione neurale del meccanismo cognitivo di aggiornamento. Nello specifico, i dati comportamentali sono stati raccolti somministrando allo stesso campione di partecipanti sia un compito di Posner, sia un compito di distribuzione spaziale, utilizzando in entrambi i casi versioni di compito richiedenti come risposta comportamentale movimenti saccadici verso gli stimoli di riferimento. Lo scopo iniziale di questo studio era quello di convalidare l'utilizzo di queste due varianti comportamentali nell'evidenziare i marker comportamentali dei meccanismi di aggiornamento dei corrispettivi modelli mentali (ossia, rispettivamente, la predittività del cue, trial dopo trial, e la distribuzione spaziale del posizionamento degli stimoli). Secondariamente, sono state investigate possibili associazioni tra i meccanismi di aggiornamento rilevati tramite i due compiti. Tuttavia, nonostante i nostri risultati abbiano confermato l'adeguatezza di tali versioni comportamentali, non sono state trovate specifiche correlazioni tra le due prestazioni.

In generale, le presenti evidenze fanno luce su aspetti tuttora discussi, riguardanti i processi attenzionali di orientamento e riorientamento spaziale e di aggiornamento dei modelli interni.

ABSTRACT

In the last twenty years, considerable research has been encouraged by the concept of two distinct attention networks in the human brain for the voluntary deployment of attention and the reorientation to unexpected events, respectively. Despite the general agreement about the main crucial nodes constituting the two networks (i.e., a dorsal network for goal-directed allocation of attention, DAN, and a ventral network for reorienting attention, VAN), some aspects are still waiting for clarification, mainly regarding each region's specific contribution and the interplay between the two networks for flexible attentional control.

With this work, therefore, we tried to elucidate these still unresolved issues by exploiting novel and avant-garde behavioral and functional approaches.

In the first study, Event-Related Optical Signal (EROS) data were collected from participants performing a detection task of a Posner-like paradigm with the aim of characterizing the spatiotemporal dynamics of attentional processes and examining the predictive interactions between and within the two attention systems.

Functional analyses, which were complemented by Granger Causality Analysis, revealed a recursive predictive interplay between definite dorsal parietal regions and visual areas subserving both attentional orienting and reorienting. Furthermore, a specific contribution of the left ventral network was found in allocating attention after the occurrence of a central predictive cue. In contrast, the right ventral network activity could reflect post-perceptual updating of the internal task-related expectations. This result is specifically derived from the investigation of the right temporoparietal junction (rTPJ), which stands for one of the most essential hubs of the VAN. Accordingly, the second study was conducted in order to better understand the implication of the rTPJ in visuospatial attentional processes. More precisely, we applied neuronavigated repetitive transcranial magnetic stimulation (rTMS, three pulses at 20 Hz per trial) over rTPJ while administering a cued discrimination task of a Posner-like paradigm. We were thus enabled to interfere online with rTPJ activity and observe potential behavioral effects related either to the reorienting process or to the mechanism of updating internal predictions about cue-target associations on a trial-by-trial basis. Behavioral analyses corroborated

our first study results: rTPJ seems to be involved in the capability of updating internal models contextually linked to task contingencies.

Consequently, the last study of this work concerns the investigation of the behavioral implementation of the updating mechanism. More precisely, behavioral data were collected from the saccadic version of both a Posner paradigm and a Location distribution paradigm in order to validate these task variants in unveiling behavioral signatures of updating mechanisms of the corresponding internal models (i.e., the trialwise cue predictability and the underlying spatial distribution of target locations, respectively). Secondly, we aimed to discover possible associations between the two updating mechanisms. However, although our findings confirmed the adequacy of our saccadic task versions, we did not find any correlational pattern between performances.

Taken together, the current findings shed light on the still debating aspects concerning visuospatial attentional orienting and reorienting and updating processes.

TABLE OF CONTENTS

GENERAL INTRODUCTION	9
EXPERIMENT 1	12
1. INTRODUCTION	12
2. MATERIAL AND METHODS	16
2.1. Participants	16
2.2. Experimental procedure	16
2.3. Behavioral Task	16
2.4. Optical recording	17
2.5. Data analysis	21
<i>2.5.1. Behavioral data</i>	21
<i>2.5.2. Functional data</i>	21
3. RESULTS	24
3.1. Behavioral results	24
3.2. Functional results	25
<i>3.2.1 Orienting process</i>	25
<i>3.2.2. Reorienting process</i>	28
4. DISCUSSION	32
4.1 Orienting	32
4.2 Reorienting	32
5. CONCLUSIONS	38
EXPERIMENT 2	40
1. INTRODUCTION	40
2. MATERIALS AND METHODS	43
2.1 Participants	43
2.2. Experimental procedure	43
2.3. Behavioral Task	44
2.4 TMS protocol	46
2.5. Behavioral data analysis	48
3. RESULTS	48
4. DISCUSSION	49
5. CONCLUSIONS	52
EXPERIMENT 3	52

1. INTRODUCTION	54
2. MATERIALS AND METHODS	57
2.1 Participants	57
2.2 Procedure and Apparatus	58
2.3 Stimuli and Experimental Paradigm	58
2.3.1 <i>Posner Cueing Task</i>	59
2.3.2 <i>Location Distribution Task</i>	61
2.4 Eye Movement Data Analysis	64
2.4.1 <i>Posner Cueing Task</i>	65
2.4.2 <i>Location Distribution Task</i>	65
2.4.5 <i>Correlations</i>	66
3. RESULTS	67
3.1 Posner Cueing Task	67
3.2 Location Distribution Task	70
3.3 Correlations	73
4. DISCUSSION	73
5. CONCLUSIONS	77
GENERAL CONCLUSIONS	78
REFERENCES	80

GENERAL INTRODUCTION

Visual attention represents a set of psychological and neural processes that regulate the processing of behaviorally relevant sensory information (Capotosto et al., 2012). Humans' daily living is indeed depicted by a multitude of visual environmental stimuli that overcome the human brain's sensory and cognitive abilities. To deal with this issue, visual attention intervenes, ruling out behaviorally irrelevant inputs while filtering behaviorally important information, giving them access to further processing. Taking into consideration the visuospatial attention framework, spatial information can be selected either endogenously or exogenously. According to the first perspective, visuospatial attention can be voluntarily deployed to specific locations or reoriented in response to novel or unexpected locations, but including important stimuli, by evaluating learned predictive contingencies between top-down cues and events (Chica et al., 2011). On the contrary, exogenous distribution of attention refers to a stimulus-driven and automatic mechanism of visuospatial orienting or reorienting to locations comprising task-irrelevant stimuli, in which any goal-directed and voluntary aspect is suppressed (Indovina & MacAluso, 2007). Moreover, besides the just-described cognitive operations of orienting and reorienting, the attentional system is implicated in a constant evaluation of the environment in order to create mental models based on current perceptions and past experiences (Friston & Kiebel, 2009). Importantly, when these models are no longer appropriate for representing specific contexts and filtering information, they need to be updated, corresponding to a post-perceptual attentional mechanism.

The starting point of this work corresponds to the well-known and significant model proposed by Corbetta and Shulman more than a decade ago, suggesting the idea of two anatomically and functionally distinct attention systems (Corbetta & Shulman, 2002). Considering spatial contexts, a dorsal frontoparietal system was indicated as responsible for top-down voluntary allocation of attention towards specific locations. In contrast, a ventral frontoparietal system was proposed to be involved in detecting stimuli occurring in unexpected locations and triggering shifts of attention. Although the identification of most of the critical hubs is widely accepted,

some crucial questions are still unresolved, especially concerning each node's specificity for attentional processes and how the two networks interact with each other (Vossel, Geng, et al., 2014). Hence, the main goal of this thesis consists of exploring the spatiotemporal dynamics of cognitive mechanisms underlying endogenous visuospatial attention covertly modulated (i.e., in the absence of head or eye movements). Indeed, we developed three experiments aimed at tackling the literature gap by employing innovative and complementary methodologies. Importantly, a common behavioral aspect was considered, namely the employment of the Posner paradigm (Posner, 1980). The latter, indeed, depicts the most suitable behavioral tool, among several attentional tasks, to disentangle attentional orienting and reorienting and to pinpoint potential post-perceptual cognitive mechanisms, linked to the attentional performance.

More specifically, in the first study, availing of a comprehensive approach, which combines the use of the Posner paradigm with the Event-Related Optical Signal technique and proper functional analyses, we studied the temporal unfolding of the posterior nodes of both attentional networks segregating activations related to the main visuospatial mechanisms (i.e., the orienting and reorienting of endogenous attention), but also highlighting the potential interplays between their neural correlates.

In the second study, taking advantage of the utilization of Transcranial Magnetic Stimulation (TMS) along with manipulation of the behavioral paradigm employed in the first experiment, we could explore the functional role of the right temporoparietal junction (rTPJ), i.e., one of the main regions included in the attentional networks, in supporting visuospatial processes. Indeed, the TMS technique enables the direct study of the engagement of specific cortical regions, interfering with their usual activity.

Finally, the third study was planned with the aim of examining the ability to update one's internal models from a behavioral standpoint. Indeed, two behavioral tasks were designed and administered. Afterward, the relative behavioral outcomes were compared in order to define the behavioral signatures of updating mechanisms.

On the whole, the studies outlined in the present work allow to go beyond the current literature, refining and extending the existing knowledge of the behavioral and neural bases of attentional processes.

EXPERIMENT 1

1. INTRODUCTION

Endogenous allocation of attentional resources in the spatial domain refers to the ability to prioritize and selectively attend to locations, including behaviorally relevant events. More specifically, during endogenous orienting, visuospatial attention is controlled by a goal-directed behavior and voluntarily focused on regions of space containing salient stimuli. Likewise, when behaviorally significant events occur in unexpected locations, visuospatial attention is reoriented toward them, establishing what is called attentional reorienting. A large number of studies have explored the brain regions serving attentional orienting and reorienting (Corbetta et al., 2000; Corbetta & Shulman, 2002; Downar et al., 2001), proposing the existence of two distinguishable, although intertwined, frontoparietal cortical systems: a dorsal and a ventral frontoparietal network (DAN and VAN, respectively). These networks emerge to be both anatomically segregated and functionally dedicated to different processes of visuospatial attention (Vossel, Geng, et al., 2014): DAN is bilaterally organized and comprises the superior parietal lobule (SPL), the intraparietal sulcus (IPS) and the frontal eye fields (FEF). In contrast, VAN is deemed more right-lateralized and comprises the temporoparietal junction (TPJ) and the ventral frontal cortex (with particular reference to the middle frontal gyrus, MFG, and the inferior frontal gyrus, IFG) (Corbetta et al., 2008). From a functional standpoint, DAN is thought to generate and carry on the cued voluntary deployment of attention. In contrast, VAN is supposed to be responsible for reorienting visuospatial attention to unexpected behaviorally relevant locations (Corbetta & Shulman, 2002).

Despite their extensively demonstrated specialization, DAN and VAN do not operate in isolation but interact to render orienting and reorienting mechanisms efficient. Besides the anatomical linking between DAN and VAN, which is assumed to be subserved by different white matter tracts as the superior longitudinal fasciculus (SLF, Mengotti et al., 2020) and the parietal inferior-to-superior tract (PIST, Catani et al., 2017), a clear understanding of the collaborative contributions of both networks is still lacking. Transcranial magnetic stimulation (TMS) studies

(Ahrens et al., 2019; Capotosto et al., 2012; Chica et al., 2011) have ascribed both endogenous orienting and exogenous reorienting to right IPS. In contrast, right TPJ has been found to be crucially involved in attentional reorienting to unattended but task-relevant stimuli only.

Moreover, by means of effective connectivity methods, imaging studies revealed significant connectivity between the right IPS and right TPJ during cued visuospatial tasks (Vossel et al., 2012; Wen et al., 2012). In addition to Vossel et al. (2009) highlighting right SPL activation in response to invalid cued targets in a location-cueing paradigm, Proskovec et al. (2018) observed functional involvement of bilateral SPL contrasting invalid against valid targets in a magnetoencephalography (MEG) study. Therefore, albeit different attentional subprocesses are selectively managed by either DAN or VAN, the current literature supports the need for a flexible and dynamic interaction to accomplish an effective attentional performance.

Furthermore, attentional processes are not neurally implemented in fronto-parietal and ventral regions only; instead, striate and extrastriate visual areas are implicated in these cognitive mechanisms as well (Chica et al., 2013). In line with this concept, previous research has shown the engagement of visual areas (i.e., cuneus) in anticipatory deployment of attention (Simpson et al., 2011) and the development of directed attentional effects from fronto-parietal regions to visual areas during location-cueing paradigms (Bressler et al., 2008; Vossel et al., 2012).

Nevertheless, although there is considerable evidence about the existence of an interaction between DAN and VAN along with the contribution of sensory regions during attentional tasks (Mengotti et al., 2020), more needs to be understood about the temporal dynamics of this interplay. To clarify the exact contribution of each node of these networks and how they predictively dialogue with each other constitutes a still unanswered question, especially as regards the attentional reorienting process. Right TPJ is traditionally considered the cortical hub of reorienting mechanisms. Yet, it has been related to multiple and different cognitive functions, leading to a heated debate with regard to its precise functional role and if it is fostered by either a functional specialization ("Fractionation view" Krall et al., 2015) or a unique shared cognitive mechanism ("Overarching view" Schuwerk

et al., 2021). Likewise, shedding light on the functional contribution of the right TPJ in supporting attentional processes still represents a critical issue. At first, right TPJ was hypothesized to be involved in the reorienting mechanism by acting as an early circuit-breaking module which interrupts the ongoing deployment of attention carried out by the DAN and enables the latter to reorient attention toward unexpected but task-relevant stimuli (Corbetta & Shulman, 2002). Nonetheless, more recent and varied results have ruled out this theory. One of the most accredited hypotheses firstly bolsters a later functional activation of right TPJ compared to the DAN (Geng & Vossel, 2013), thus sustaining the opposite time scenario of the circuit-breaking theory. Secondly, it endorses the association between the right TPJ and the P3b (a sub-component of the electrophysiological potential P300), which usually occurs in a late post-target time window (300-500 ms). Specifically, given that the P3b is considered a neurophysiological correlate of contextual updating (Donchin & Coles, 1998; Polich, 2007), which is usually elicited after the beginning of reorienting (Mengotti et al., 2017), the right TPJ should play a post-perceptual role by updating internal models of the attentional context to generate and guide proper expectations and actions (Geng & Vossel, 2013).

This possibility is corroborated by the results of a previous work (Parisi et al., 2020) using fast optical imaging data. In this study, the authors unraveled functional relationships among cortical brain areas during endogenous orienting and reorienting, which was pointed out through a modified visuospatial version of the Posner paradigm (Posner, 1980). Participants performed a discrimination task in which they were asked to discriminate the orientation of a peripheral target occurring after presenting a central informative cue (i.e., an arrow). Notably, the cue direction was consistent throughout a single block, that is, to the right (in half of the blocks) or the left (in the other half of the blocks) hemifield, while the order of the blocks was alternated. Trials could be valid (75%) when the cue indicated the hemifield in which the target occurred or invalid (25%) when the target appeared in the uncued hemifield. With regard to the reorienting mechanism, which was studied by analyzing invalid trials, the authors showed a later and recursive functional recruitment of the right TPJ. They indeed suggested an early mutual interaction between visual and dorsal regions, which seems responsible for the

different attentional sub-operations (i.e., encoding of the mismatch between expectation and reality, disengaging attention from the cued location and triggering reorientation to the target) and communicates to the right TPJ only at later timeframes, accordingly ascribing to it a post-perceptual role in updating the preexisting internal model instead of triggering the reorienting process. Noteworthy, the Posner paradigm constitutes an excellent behavioral model to investigate attentional orienting and reorienting and to further disentangle the latter from updating processes (Arjona Valladares et al., 2017; Käsbauer et al., 2020).

In the present study, we thus aimed at describing the neural spatiotemporal dynamics of visuospatial attentional processes by manipulating the paradigm employed in Parisi et al. (2020), seeking to return it as similar as possible to its classical visuospatial version proposed by Posner: we indeed administered a simple detection task instead of a discrimination task, and we implemented a random cue indicating toward either the left or the right hemifield instead of showing a consistent cue within a single block. By means of these manipulations, we intended to study attentional processes with the lowest cognitive demand in order to trace the time-course of brain activations in the posterior nodes of the DAN and VAN, with particular reference to cast light on right TPJ recruitment and to point out their different roles by exploring the predictive relationships among them.

Finally, functional data were collected by means of the Event-Related Optical Signal (EROS) or Fast Optical Signal (FOS) (Chiarelli et al., 2013, 2014; Gratton et al., 1995; Gratton & Fabiani, 2001), which stands for an innovative approach characterized by both a high temporal localization power of less than 50 ms (Baniqued et al., 2013) and a good spatial localization power (the latter undoubtedly superior to EEG and MEG measurements) representing an optimal methodology to obtain valuable new insights into the time-course of attentional processing in parallel with precise identification of cortical regions which emerge activated throughout the processes at hand.

2. MATERIAL AND METHODS

2.1. Participants

Thirty healthy volunteers were recruited for the study (8 males). Their ages ranged between 20 and 37 years (mean age \pm standard deviation: 24.7 ± 3.4), and they were all right-handed, as assessed with the Edinburgh Handedness Inventory (Oldfield, 1971). All reported normal or corrected-to-normal vision and no history of neurological or psychiatric disorders. All but one (author E.C.) were naïve to the purposes of the study. All participants gave their written informed consent before participation, which was refunded. The Ethics Committee of the Verona Azienda Ospedaliera Universitaria Integrata (AOUI) approved the study, which was carried out according to the principles laid down by the 2013 Declaration of Helsinki.

Data from 3 participants were excluded from the analysis as being behavioral task outliers. Moreover, data from another participant were discarded because of digitization issues. Thus, the final sample comprised twenty-six participants (7 males, mean age \pm standard deviation: 23.7 ± 2.4).

2.2. Experimental procedure

To prevent tiredness and to achieve an acceptable number of trials, participants performed two distinct experimental sessions held over two days. There were no differences between them in setting and behavioral conditions, excluding EROS montages (see below). Each session lasted about three and a half hours and consisted of EROS setup, optical data recording during the behavioral task, and co-registration procedures (i.e., the digitization of optode scalp locations).

2.3. Behavioral Task

Participants were individually tested in a dimly lit testing room. During the experiment, they sat in front of a 17-inch LCD monitor (resolution 1920x1080, refresh rate of 144 Hz) placed at a viewing distance of 57 cm with head position stabilized by an adaptable chin rest so that eyes could be adjusted to the center of the screen.

A cued detection task was administered (Posner, 1980). Stimuli were generated using E-Prime 2.0 software (E-Prime Psychology Software Tools Inc., Pittsburgh,

PA, USA) and consisted of vertical or horizontal, black-and-white, 2° square gratings. Participants were instructed to maintain fixation on a centrally presented black cross, which 500 ms later was followed by a predictive random cue above the fixation cross (duration 200 ms). After a random interval, ranging from 300 to 600 ms, the target was presented for 150 ms at an eccentricity of 2° from the fixation cross to the inner edge along the horizontal meridian. Each stimulus of a single trial was displayed on a grey background (see Fig. 1A). Participants were to respond as fast as possible to the target by pressing the space bar of the keyboard with the index finger of their right hand in half of the blocks, alternating with the index finger of their left hand in the other half (the order of the hand was counterbalanced across both blocks and participants). Participants were both asked to deploy attention to the side indicated by the cue and informed about its general predictive value.

In each block, horizontal and vertical gratings randomly occurred with the same probability to avoid habituation. Moreover, trials could be valid (75%), that is, when the target appeared on the side indicated by the cue, or invalid (25%) when the target appeared on the opposite uncued side.

Each experimental session was composed of 24 blocks (for a total of 48 blocks per participant). Each block consisted of 48 valid trials, 16 invalid trials, and 16 catch trials (no target after the cue presentation) for a total of 3840 trials (2304 valid, 768 invalid, and 768 catch trials) per participant.

Participants could rest during inter-block intervals and initiate the next block by pressing a key.

2.4. Optical recording

Simultaneously with behavioral data acquisition, brain activity was recorded by means of two synchronized frequency domain oximeters (Imagent, ISS, Inc., Champaign, IL). Near-infrared light (830 nm) was emitted by thirty-two laser diodes, modulated at 110 MHz. The light was directed to the participant's head through 400 μm optic fibers and then detected by eight 3-mm fiber-optic bundles connected to photomultiplier tubes (PMTs). The detectors were modulated at a slightly different frequency in relation to laser diodes, generating a signal with a 3125 Hz cross-correlation frequency. PMTs' output current was then processed by

Fast Fourier Transform to obtain measures of the signal's DC intensity, AC amplitude, and relative phase delay (source to detector). Only changes in phase delay data (converted into picoseconds delay) were examined in this study. The phase delay parameter is indeed more interesting for deriving images of brain activity with high spatial and temporal resolution than the other two optical measures (i.e., DC and AC) (Gratton et al., 2010).

Custom-built helmets, available in two sizes, were used to secure all sources and detector fibers on each participant's head. For each size, two different configurations were exploited, one per experimental session, and then combined to maximize coverage of the occipital and posterior temporoparietal cortices (See Fig. 1B). In each montage, sources and detectors were arranged to allow each detector to detect light from up to 16 time-multiplexed sources and to enable sources to emit light concurrently, avoiding cross-talks between channels. Depending on this time-multiplexing method, sources were sequentially switched on for 1.6 ms and switched off for 24 ms in each specific multiplexed set. This achieved a 25.6 ms lasting cycle and a sampling rate of 39.0625 Hz. Optical data were acquired from a total amount of 128 channels, even though only channels with source-detector distances ranging between 17.5 and 50 mm were considered. Longer or shorter distances were excluded because, considering the first ones, optical signals could be unreliable, while shorter channels could measure light unable to reach the cerebral cortex.

Nineteen participants underwent structural MRI scans in a 1.5 Tesla Philips scanner at the Borgo Roma Hospital in Verona. A standard 15-channel head coil was employed, and 3D T1-weighted MR images were acquired with a magnetization-prepared rapid acquisition gradient echo (MPRAGE) sequence. Data acquisition parameters were as follows: phase encoding direction= anterior to posterior, voxel size= 0.5 X 0.5 X 1 mm, Repetition Time= 7.7 ms, Echo Time= 3.5 ms, field of view= 165x 512 x 512 mm, flip angle= 8°.

For the remaining seven participants, structural MRI was not available, so an estimated MR-based head model was individually created using the SofTactic system (SofTactic, E.M.S., Bologna, Italy) combined with a 3D optical digitizer (Polaris Vicra, NDI, Waterloo, Canada). A warping procedure was employed based

on four fiducial points (nasion, inion, and pre-auricular points) and a large number of scalp points corresponding to the holder positions of each helmet (247 and 259 points, respectively). Based on the scalp points digitization, a proper procedure generated a virtual reconstruction of the scalp surface. This reconstruction was then used to compute 345 scalp reference points based on the international 10–5 system (a set per participant) through which the averaged standard template MRIs were adjusted (Mazzi et al., in prep.). Following each EROS session, every source and detector holder location on the helmet, as well as fiducial points (nasion, inion, and pre-auricular points), were digitized for each participant. The digitized scalp locations were co-registered with the structural MR images or the estimated MRI using a specific procedure performed in the OCP software package (Optimized Co-registration Package, MATLAB code). The co-registration procedure (Chiarelli et al., 2015), essentially based on fiducial alignment processes (Whalen et al., 2008), was identical for both the MRI types. Finally, co-registered individual data were transformed to MNI space for the following analyses.

Optical data were collected by means of the ISS Corporation "Boxy" program and subsequently preprocessed using an in-house MATLAB-based software, namely P-POD (Pre-Processing of Optical Data). Data were corrected for phase wrapping, de-trended to remove drifts, and baseline corrected. Afterward, the time delay was obtained by converting the phase into picoseconds, adjusted to zero for each block. Later on, pulse artifacts were removed (heartbeat rate range 45-200), and data were band-pass filtered to remove frequencies outside the 0.5-15 Hz range. Finally, output data were segmented into epochs time-locked either to the cue or the target onset and then averaged for each time point, channel, condition, and participant separately. The length of the epochs was thus the same for each EROS contrast (see below section 2.5.2.1. EROS analysis), namely 1484 ms.

Statistical analyses of optical data were computed using the Opt-3d custom software package (Gratton, 2000). Mean optical signals were obtained by averaging those originating in channels whose diffusion paths converged in a given voxel (Wolf et al., 2014). Phase delay data were baseline corrected using either a 200 ms pre-target interval or a 200 ms pre-cue interval (according to the analysis taken into consideration) and spatially smoothed with an 8-mm Gaussian kernel. Group-level

t-statistics were calculated across participants and then converted to z-scores for each voxel at each time point. Z-score maps were thus computed from the p-value for each t-test and underwent the proper correction for multiple comparisons based on random field theory (Kiebel et al., 1999; Worsley et al., 1995). Eventually, according to the physical homogenous model (Arridge & Schweiger, 1995; Gratton, 2000), Z-scores were weighted and orthogonally projected onto a template MNI brain's coronal, sagittal, or axial surfaces.

ROIs for the statistical analysis were identified by selecting those areas hypothesized to show attentional control modulation within areas included in EROS coverage (Fig. 1C). ROIs thus comprised occipital regions, i.e., V1 and the dorsal portion of the cuneus, dorso-parietal regions, i.e., left and right SPLs (l/rSPL) and left and right IPSs (l/rIPS, representing the posterior portion of the DAN), and ventral regions, i.e., left and right TPJs (l/rTPJ, representing the temporo-parietal portion of the VAN). Specific ROIs coordinates were selected by matching anatomical coordinates of parietal, temporal, and occipital areas previously used in literature (e.g., Baniqued et al., 2018; Parisi et al. 2020) and the correspondent Brodmann areas incorporating these regions (i.e., BA17 for V1, BA 18 and 19 for cuneus, BA7 for SPL, the intersection of BA7 and BA39 for IPS, BA39 for TPJ). Moreover, a potential overlapping of ROIs boundaries was eliminated by referring to the Bioimage Suite Web (<https://bioimagesuiteweb.github.io/webapp/mni2tal.html>). A 2-dimensional box-shaped structure described ROIs considered in this paper (the absence of the third dimension is due to the projection of the optical signal to the brain surface). Indeed, ROIs were examined availing of axial (x,y), sagittal (y,z), or coronal projections (x,z) only (see Table 1).

Table 1. MNI coordinates of selected ROIs

Region	Projection	Coordinates	Involved BA
Right SPL	Axial	x = 0 20 y = -84 -64	7
Left SPL	Axial	x = -20 0 y = -84 -64	7
Right IPS	Axial	x = 26 40 y = -87 -59	7-39
Left IPS	Axial	x = -36 -22 y = -87 -59	7-39
Right TPJ	Sagittal	y = -69 -49 z = 21 41	39
V1	Coronal	x = -10 10 z = -4 16	17
Cuneus	Coronal	x = -10 10 z = 20 40	18-19

2.5. Data analysis

2.5.1. Behavioral data

Data were processed using MATLAB 2021b and analyzed with Jamovi for Windows, version 1.6.23.

Reaction times (RTs) were evaluated to explore behavioral data. In each condition, anticipations (RTs < 150 ms) and responses deviating > 3SDs from the mean were excluded from the analyses. Mean RTs and the corresponding standard deviations (SDs) were measured for each of the four behavioral conditions (right target valid – invalid, left target valid – invalid) across participants, independently from target orientation (vertical or horizontal).

A repeated-measures analysis of variance (ANOVA) was then conducted on mean RTs, with the *target side* (right/left) and *cue side* (right/left) as within-subject factors. Where needed, Bonferroni-corrected post-hoc t-tests were applied.

2.5.2. Functional data

2.5.2.1. EROS analysis

The change in phase delay from baseline was the dependent variable for optical data analyses, averaged for each subject, condition, and time point. Specifically, one-tailed tests were performed on each ROI's average at each latency. Statistical significance was measured by ROI peak Z scores with $p < 0.05$, adjusted for multiple comparisons (Kiebel et al., 1999; Worsley et al., 1995). Concerning statistical analyses, trials were collapsed independently from target orientation, and three

main contrasts were selected: all (valid and invalid) versus baseline, valid versus baseline, and invalid versus baseline.

For the first contrast (all versus baseline), all trials were collapsed together and contrasted against baseline, namely the 200 ms time window preceding cue onset. To observe the orienting process after the cue onset, we analyzed latencies ranging between 0 ms and 307 ms (where 0 ms corresponds to the cue onset). Indeed, since cue occurrence typically triggers attentional deployment processes and our cue-target interval was variably randomized among trials (from 300 to 600 ms after the cue onset), in our pre-target analysis, we chose that specific time window considering that the latencies later than 300 ms after cue onset would not be homogenous to the orienting response because of the target presence in part of the trials.

For the other two contrasts (valid versus baseline and invalid versus baseline), valid and invalid trials were separately contrasted against baseline (the 200 ms preceding the target onset), independently from the visual hemifield where the target occurred. Functional activity was evaluated from 0 ms to 650 ms (0 ms corresponds to the target onset).

2.5.2.2. *Granger causality*

Forward GCA was calculated to characterize the directed functional interaction among activations in different regions at different time lags. The central idea underlying GCA is that directional influence from a specific region to another one, subsequent in time, can be deduced if past signal values of the first brain region support the prediction of that temporally later region's present and future signal values. Therefore, identifying significant seeds within different ROIs is needed to perform GCA. A single seed consists of a time window whose predictive flow will be evaluated comparing it to another window of the same duration. In a nutshell, this approach investigates whether the activity of the seed ROI predicts the activity in the other ROIs at a later time at the individual level, thus providing the opportunity to highlight complex patterns across participants that conventional EROS analyses may not reveal. Statistical maps, which were obtained from the average of individual values calculated separately per ROI and contrast, were

generated by means of the computation of t statistics and transformation into z scores. This procedure was conducted for each time lag. Subsequently, a correction for multiple comparisons within each ROI was performed using the same random field theory techniques (Kiebel et al., 1999; Worsley et al., 1995) used for EROS analysis. Directed functional interactions were studied at lags divided by 25.6 ms intervals (i.e., the sampling rate), proceeding from a lag of 0 ms until a lag of 358 ms, for a total of 15 time lags (which correspond to the same time points employed in EROS analyses). Statistically significant predicted ROI peaks were detected when z-scores exceeded the criterion value $p < .05$ at each specific lag, which, however, did not correspond to the actual timing of activation of the predicted ROI. Accordingly, we found the significant time window by adding the number corresponding to the significant time lag (i.e., from 1 to 15) to the starting seed interval. The resulting time window was applied to the predicted ROI activation timeframe. The timing of the most significant ROI peak in the resulting time interval consisted of the actual activation timing of the predicted ROI. The critical time window designated for each contrast started from the target onset onwards for valid and invalid versus baseline contrasts. Instead, the time points corresponding to the 300 ms after cue onset were considered for the all versus baseline contrast. After focusing on lags in keeping with EROS results, exploratory analyses were run to examine additional predictive effects. We indeed decided to adopt a specific procedure to perform GCA: ROIs utilized as seeds corresponded to both ROIs exhibiting significant activations in EROS analyses and ROIs whose activity was predicted by previous in-time seeds

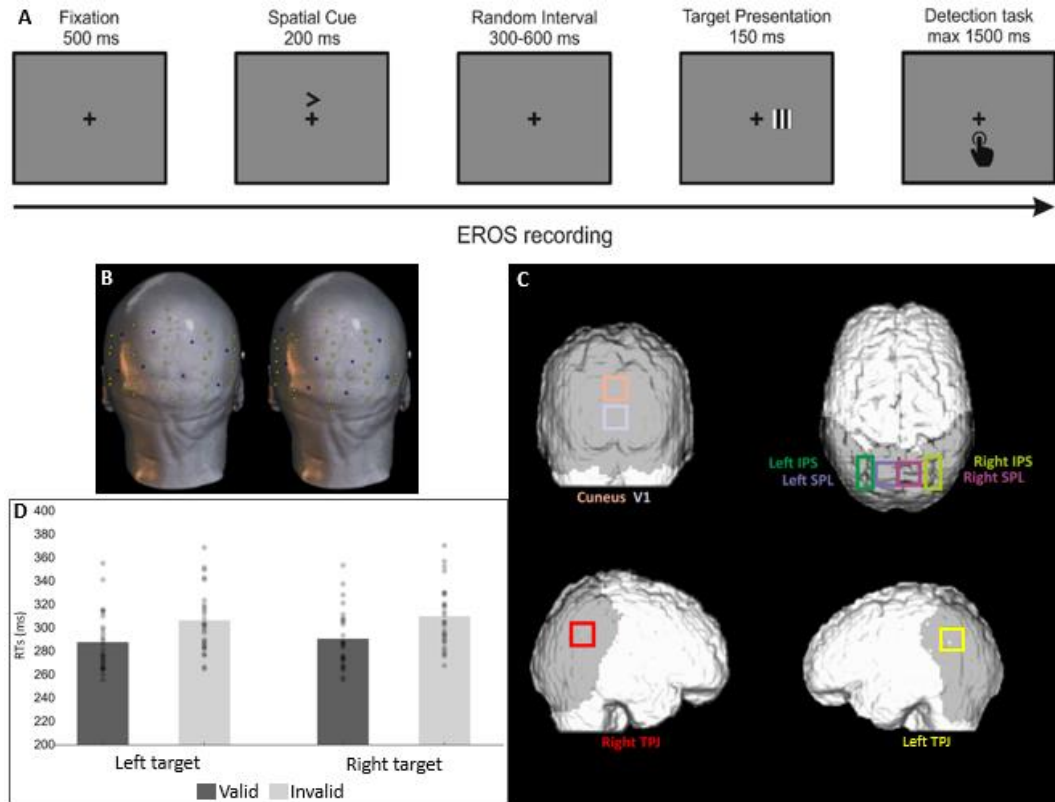


Figure 1. Method and behavioral results.

(A) Experimental paradigm. A fixation cross was presented for 500 ms followed by a central predictive cue lasting 200 ms. After a random interval ranging from 300 to 600 ms, the visual target occurred (for 150 ms) giving participants 1500 ms to respond to it. In this example, a valid trial is displayed (i.e., the cue indicates to the same visual hemifield in which the target is subsequently presented). (B) Optical montages. Two recording montages were used for each helmet size. Infrared optical sources (yellow dots) and detectors (blue dots) were placed to maximally cover the parietal and occipital cortices. Here, source and detector locations are plotted on the anatomical scan of a representative participant (Parisi et al., 2020). (C) Selected ROIs. Estimated boundaries of the selected ROIs used for EROS and GCA analyses. ROIs are displayed in coronal (visual regions), axial (dorsal regions), and sagittal (ventral region) views. ROIs coordinates are listed in Table 1. (D) Behavioral results. Mean response times are plotted as a function of whether the target appeared in the right or left hemifield and a function of whether the attention cue was valid or invalid. For each condition, individual data are plotted (grey dots) along with averaged values

3. RESULTS

3.1. Behavioral results

The ANOVA executed on mean RTs did not show a significant main effect of either the target side ($F_{(1,25)} = 3.957$, $p < 0.058$, $\eta^2_p = 0.137$) or the cue side ($F_{(1,25)} = 0.611$, $p < 0.442$, $\eta^2_p = 0.024$). In contrast, it revealed a significant interaction between the target side and the cue side ($F_{(1,25)} = 67.460$, $p < 0.001$, $\eta^2_p = 0.730$). Accordingly, Bonferroni-corrected post-hoc t-tests indicated that mean RTs for right valid trials were statistically different compared to mean RTs for right invalid trials ($tp < 0.001$). Likewise, mean RTs for left valid trials were shown to be statistically different

compared to mean RTs for left invalid trials ($p < 0.001$). On the contrary, the RTs comparisons between left valid trials and right valid trials and between left invalid trials and right invalid trials did not reveal any statistically significant difference. These results suggest a highly reliable attentional orienting advantage in target detection: on the one hand, the valid condition always yields faster RTs; on the other hand, the target side factor did not modulate cue-related performances.

3.2. Functional results

3.2.1 Orienting process

Two EROS contrasts were carried out to explore the spatiotemporal dynamics underlying attentional orienting. Specifically, the all versus baseline contrast (Fig. 2A, after cue onset) was conducted in the time window ranging from the cue onset to 300 ms post cue. In contrast, the valid versus baseline contrast (Fig. 2B, after target onset) considered the time window from target onset to 650 ms post-target.

3.2.1.1. After cue onset

Concerning the all versus baseline contrast, there was an increase of activation in both ISPL ($z = 2.76$; $z_{crit} = 2.68$) and the dorsal portion of the cuneus ($z = 3.27$; $z_{crit} = 2.77$) at 102 ms after the cue onset. The dorsal portion of the cuneus showed greater activity at 127 ms after the cue onset as well ($z = 2.79$; $z_{crit} = 2.63$). At the same latency, we further observed greater activity occurring in rSPL ($z = 2.75$; $z_{crit} = 2.72$). Subsequently, at a latency of 307 ms after the cue onset, a significant increase of activation was found in ITPJ ($z = 2.94$; $z_{crit} = 2.67$). See Fig. 2A.

3.2.1.2. After target onset

Comparing valid trials to the baseline condition, we found a significant increase of activation in the dorsal portion of the cuneus at 255 ms ($z = 2.90$; $z_{crit} = 2.74$) after target onset. Moreover, significant activity was found in ISPL activation at a latency of 332 ms ($z = 2.45$; $z_{crit} = 2.39$) after target onset.

Importantly, the functional results from both contrasts corroborate the concept pointed out by previous evidence about the involvement of both bilateral dorso-parietal and visual areas in attentional orienting. See Fig. 2B.

3.2.1.3. Granger Causality - After cue onset

GCA was conducted to deepen orienting and reorienting neural dynamics by investigating the directed functional influences among cortical regions in the attentional dorso-parietal and ventro-parietal networks.

GCA applied to the all versus baseline contrast allowed us to explore the stream of predictive influences straight after cue occurrence. In particular, the significant EROS activity in cuneus, peaking at 102 ms after the cue onset, was predictive of activity in ISPL corresponding to a peak at 307 ms. Moreover, peak activation of 127 ms in rSPL predicted peak activation in ITPJ at 307 ms after the cue onset (see Table 2 for significant lags and the corresponding time windows). As a result, a predictive dialogue among visual and dorsal areas emerged along with a predictive relationship between dorsal and ventral regions (see Fig. 2C and Table 2 for significant lags, the corresponding time windows, and statistics).

3.2.1.4. Granger Causality - After target onset

By applying GCA to the valid versus baseline contrast, we could investigate predictive relationships between our ROIs in the time window after target onset. The stream of predictive influences began from activity in cuneus, which was predictive of activity in IIPS (peak activation 358 ms), rSPL (peak activation 435 ms), and V1 (peak activation 537 ms). The former predicted ROI (i.e., IIPS peaking at 358 ms) was, in turn, predictive of activity in rTPJ (peak activation 383 ms) and V1 (peak activation 614 ms), while rSPL predicted orienting activity in IIPS at a later lag inferring peak at 639 ms (see Fig. 2D and Table 2 for significant lags, the corresponding time windows, and statistics).

GCA applied to the valid versus baseline contrast displays results analogous to those of the all versus baseline contrast, indicating a bilateral dorsal-parietal and visual areas engagement, mainly characterized by bi-directional predictive connections between dorsal and visual area activations.

The prediction of rTPJ from a seed detected in IIPS, in the valid versus baseline contrast, appears to be an uncommon outcome. RTPJ does not seem to have a specific role in this process, mainly because it, in turn, does not predict any other ROIs subsequent significant activation, thus revealing mere functional connectivity between these areas but not effective connectivity, i.e., related to the task at hand.

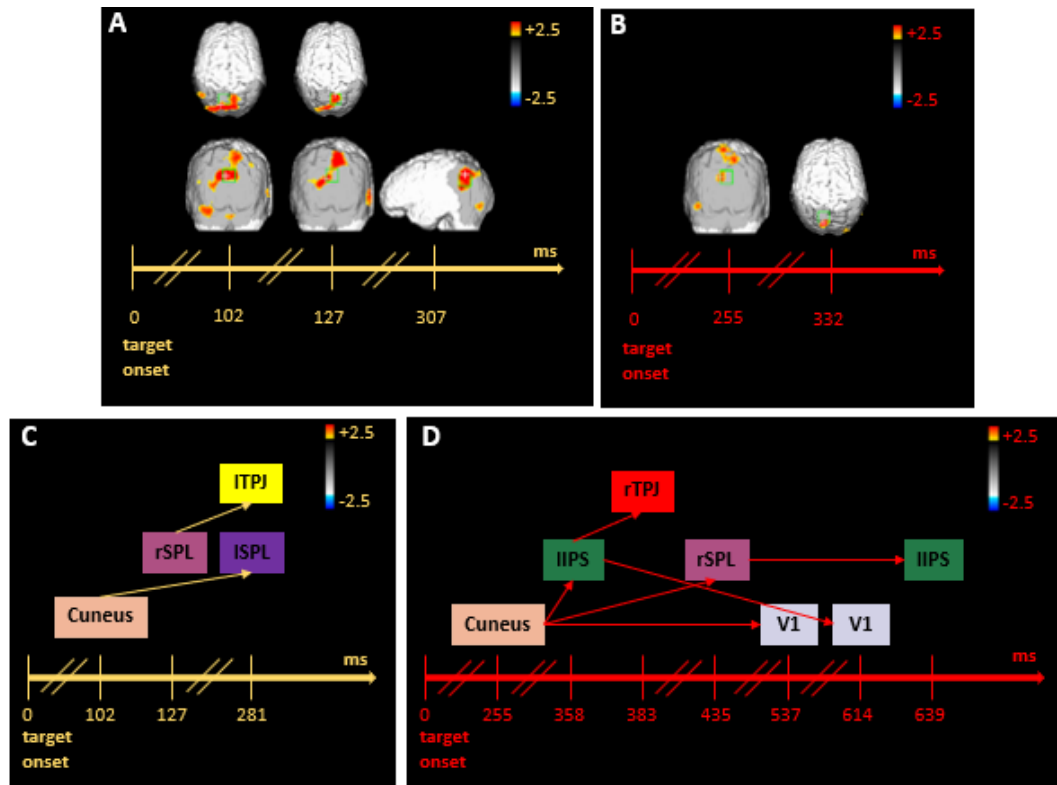


Figure 2. EROS orienting effects and Granger results.

(A) EROS orienting effects after the cue onset. Significant statistical parametric maps of the z-score difference between all trials and baseline (corresponding to the 200 ms time window preceding the cue onset) are illustrated (activation threshold z-score = 2.0). Each map constitutes a 25.6 ms interval, within the 307 ms after the cue onset, in which significant effects occurred in selected ROIs (green boxes). The peak voxel is shown by the white cross within each ROI. (B) EROS orienting effects after the target onset. Significant statistical parametric maps of the z-score difference between valid trials and baseline (corresponding to the 200 ms preceding the target onset) are illustrated (activation threshold z-score = 2.0). Each map constitutes a 25.6 ms interval of 650 ms after the target onset, in which significant effects occurred in selected ROIs (green boxes). The peak voxel is shown by the white cross within each ROI. (C) GCA results of all versus baseline contrast. (D) GCA results of valid versus baseline contrast. For GCA analyses all dorsal and visual ROIs were chosen as seeds at different time lags. Here, each colored box corresponds to a specific ROI. Each arrow indicates a significant predictive link between the starting box/seed/ROI at a specific time lag and the matching box that depicts the predicted ROI at a subsequent time lag (see Table 2). The values indicated on the timeline refer to the peak activity for each ROI, within the considered time interval.

Table 2. Granger analyses – Orienting Results

Seed ROI	Seed Interval (ms)	Peak Activity (ms)	Predicted ROI(s) (PR)	PR Interval (ms)	PR Peak Activity (ms)	Sig. Lag	Statistics
<i>After cue onset</i>							
Cuneus	0-204	102	ISPL	204-435	307	204	$z = 3.35$ $z_{crit} = 2.94$
rSPL	51-204	127	ITPJ	25-307	307	76	$z = 2.83$ $z_{crit} = 2.71$
<i>After target onset</i>							
Cuneus	153-307	255	IIPS	281-435	358	127	$z = 3.01$ $z_{crit} = 2.97$
			rSPL	358-511	435	204	$z = 3.40$ $z_{crit} = 3.00$
			V1	386-537	537	230	$z = 3.18$ $z_{crit} = 2.90$
IIPS	281-435	358	rTPJ	281-384	383	332	$z = 3.65$ $z_{crit} = 2.88$
			V1	409-537	614	25	$z = 2.97$ $z_{crit} = 2.85$
rSPL	358-486	435	IIPS	639-767	639	281	$z = 3.22$ $z_{crit} = 3.04$

3.2.2. Reorienting process

3.2.2.1 EROS results

Invalid trials were contrasted with the baseline to unveil the neural dynamics responsible for attentional reorienting. The analyzed time window is the same as the valid versus baseline contrast.

We observed greater activity in both IIPS and ISPL at 51 ms ($z = 3.60$; $z_{crit} = 2.76$; $z = 3.26$; $z_{crit} = 2.92$) after target onset. Then, we found stronger activation in V1 and rIPS at 153 ms ($z = 3.2$; $z_{crit} = 2.47$) and 204 ms ($z = 2.49$; $z_{crit} = 2.46$), respectively. Finally, greater activity was observed in ISPL at 332 ms ($z = 2.623$; $z_{crit} = 2.62$) after target onset (See Fig. 3A). The present reorienting results seem to reveal similar dynamics compared to attentional orienting: a robust engagement of the dorso-parietal network along with visual areas. It should be noted that these findings do not indicate the recruitment of the ventral network, in particular of rTPJ, in this type of process.

3.2.2.2 Granger causality results

We availed of GCA to better understand the role of the ventral network, especially of rTPJ, and its predictive relationships with dorsal and visual areas in reorienting operations. Based on the same reasoning as the one used for previous GCA, seeds identified earlier in time revealed predictive connections so that dorsal areas predicted activity in dorsal areas only (i.e., ISPL, peaking at 51 ms, is predictive of activity in rSPL peaking at 204 ms; IIPS, peaking at 51 ms, is predictive of activity in rIPS peaking at 358 ms), and, similarly, visual areas predicted activity in visual

ROIs exclusively (i.e. V1, peaking at 153 ms, is predictive of activity in cuneus peaking at 255 and 409 ms). Subsequently, the sustained recurrent reciprocal prediction pattern between dorsal and visual areas turned out. Indeed, activity in dorsal areas was predictive of activity in dorsal and visual areas, and activity in visual areas was predictive of activity in visual and dorsal ROIs. For instance, a seed identified in rIPS at a range between 102 and 255 ms (peak activation 204 ms) predicted activity in rIPS (peak activation 358 ms) and visual areas, including V1 (peak activation both 255 and 409 ms) and cuneus (peak activation 409 ms). Moreover, activity in cuneus corresponding to a peak at 255 (which was previously predicted by V1 peaking at 153 ms) resulted in predicting activity firstly in V1 (peak activation 409 ms) and secondly in IIPS (peak activation 537 ms). Significantly, rTPJ was also involved in these attentional predictive processes. Activity in rTPJ was predicted by dorsal and visual areas at different and belated time lags. More specifically, activity in rSPL (peak activation 204) was predictive of activity in rTPJ with a peak activation at 281 ms. Furthermore, a seed identified in cuneus (peak activation 255) predicted activity in rTPJ at two later lags, inferring peaks at 511 and 588 ms (see Fig. 3B and Table 3 for significant lags, the corresponding time windows, and statistics). The main difference concerning orienting results is that in the context of attentional reorienting, rTPJ predicts, in turn, activity in visual and dorsal ROIs at subsequent lags, while in the orienting process, it does not carry on the stream of predictive influences.

Overall, these reorienting findings underline a predictive model whereby dorsal and visual areas predict themselves at an early stage. Afterward, a similar prediction pattern to that revealed in orienting GCA develops, showing a mutually predictive interface between dorsal and visual areas. Finally, the ventral network, corresponding to rTPJ, comes into play by reciprocally predicting both dorsal and visual regions.

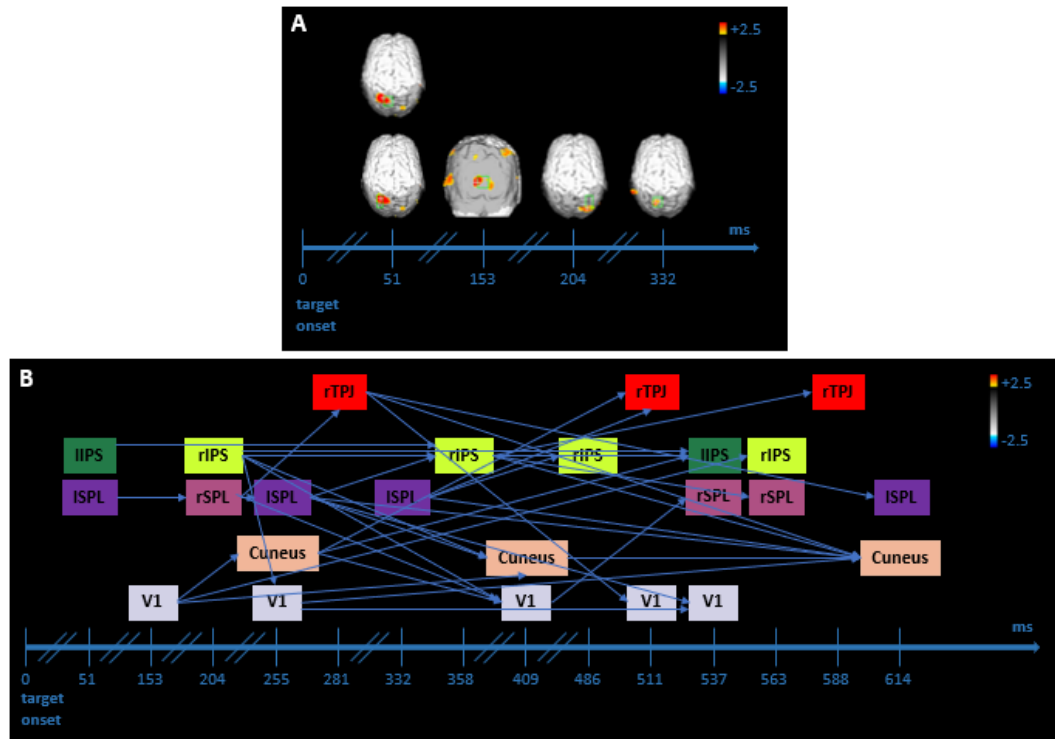


Figure 3. Reorienting EROS effects and Granger results.

(A) EROS reorienting effect after the target onset. Significant statistical parametric maps of the z-score difference between invalid trials and baseline (corresponding to the 200 ms preceding the target onset) are illustrated (activation threshold z-score = 2.0). Each map constitutes a 25.6 ms interval of 650 ms after target onset, in which significant effects occurred in selected ROIs (green boxes). The peak voxel is shown by the white cross within each ROI. (B) GCA results of invalid versus baseline contrast. Again, each arrow indicates a significant predictive link between the starting box/seed/ROI at a precise time lag, and the matching box that depicts the predicted ROI at a subsequent time lag (see Table 3). The values reported on the timeline refer to the peak activity within the considered time interval for each ROI

Table 3. Granger analyses – Reorienting Results

Seed ROI	Seed Interval (ms)	Peak Activity (ms)	Predicted ROI(s) (PR)	PR Interval (ms)	PR Peak Activity (ms)	Sig. Lag	Statistics
lIPS	0-127	51	rIPS	255-383	409	255	z= 3.46 z crit= 2.91
ISPL	0-127	51	rSPL	179-307	307	179	z= 3.13 z crit= 3.05
V1	76-230	153	Cuneus	153-307	255	76	z= 2.96 z crit= 2.85
			Cuneus	358-511	409	281	z= 2.94 z crit= 2.87
			rIPS	435-588	563	358	z= 2.87 z crit= 2.81
rIPS	102-255	204	V1	332-511	255	153	z= 3.28 z crit= 2.99
			V1	307-486	409	179	z= 3.08 z crit= 2.90
			Cuneus	409-537	409	179	z= 3.01 z crit= 2.84
			rIPS	332-486	358	230	z= 3.28 z crit= 2.99
rSPL	76-255	204	ISPL	230-409	255	153	z= 3.01 z crit= 2.98
			rTPJ	127-307	281	51	z= 3.35 z crit= 2.75
			rIPS	230-409	358	153	z= 2.75 z crit= 2.72
			V1	307-486	409	204	z= 3.04 z crit= 2.89
			lIPS	435-614	537	358	z= 2.98 z crit= 2.93
ISPL	204-307	255	rIPS	332-435	358	127	z= 3.09 z crit= 3.02
			V1	486-588	537	281	z= 4.12 z crit= 3.08
			Cuneus	563-665	614	358	z= 3.28 z crit= 3.04
V1	179-332	255	V1	511-665	537	332	z= 3.20 z crit= 3.15
			Cuneus	460-614	614	281	z= 3.13 z crit= 2.58
Cuneus	179-358	255	V1	307-435	409	127	z= 3.24 z crit= 2.81
			rTPJ	460-639	511	281	z= 3.01 z crit= 2.89
			lIPS	486-665	537	307	z= 3.15 z crit= 2.56
rTPJ	230-383	281	V1	358-511	511	127	z= 3.09 z crit= 2.84
			Cuneus	588-742	61	358	z= 2.91 z crit= 2.87
			ISPL	511-665	614/639	281	z= 2.91 z crit= 2.84
ISPL	281-383	332	Cuneus	307-409	409	25	z= 3.04 z crit= 3.03
			rIPS	409-511	486	127	z= 3.04 z crit= 2.98
			rTPJ	409-511	511	127	z= 3.56 z crit= 3.19
			Cuneus	486-639	614	204	z= 3.34 z crit= 3.20
rIPS	281-435	358	lIPS	537-691	537	255	z= 3.40 z crit= 2.89
			rSPL	563-716	563	358	z= 3.24 z crit= 2.95
			rTPJ	588-742	588	307	z= 3.17 z crit= 2.95
			Cuneus	563-716	614	281	z= 2.97 z crit= 2.96
V1	332-486	409	rSPL	409-563	537	76	z= 3.25 z crit= 3.05
cuneus	307-537	409	Cuneus	511-742	614	204	z= 3.23 z crit= 3.10

4. DISCUSSION

The purpose of the present study was to reveal the neural implementation of visuospatial attentional processes from both a spatial and temporal point of view by coupling a spatial cueing paradigm with fast optical imaging data. The former is usually characterized by the processing of valid and invalid trials. Valid trials typically engender a voluntary deployment of attention (after interpreting the predictive cue) and a cue-related orienting response, entailing distinct subprocesses: disengaging attention from the central fixation point and shifting and engaging attention to the cued location. A mismatch between the cued and actual target location is instead triggered by invalid trials, requiring further attentional mechanisms, i.e., disengaging, shifting, and re-engaging attention to the correct location (Natale et al., 2009). By availing of the EROS technique, we intended to disclose the brain regions responsible for each processing stage, developing one after another during the orienting (elicited by valid trials) and reorienting (elicited by invalid trials) processes. By integrating a good temporal localization power with a good spatial localization ability, EROS enabled us to identify the timing of our ROIs' activation over the two attentional mechanisms. Indeed, the combination of different methodologies is usually required in order to simultaneously obtain high resolution in both dimensions (i.e., space and time) without, however, fully achieving the goal because of theoretical and technical discrepancies between distinct techniques (Gratton, 2010; Luck, 1999). Furthermore, we maximized EROS potential by adding GCA to functional data analysis and unveiling the predictive and mutual interactions among the different ROIs, whose exact nature is still unclear but crucial to thoroughly understanding visuospatial attentional dynamics.

4.1 Orienting

We explored the ability to intentionally orient attention to a spatially cued, lateralized visual stimulus by considering two EROS contrasts: all trials (independently from validity conditions) versus baseline and valid trials versus baseline. The former contrast was performed in order to investigate the spatiotemporal correlates related to anticipatory visual orienting taking place across

cue-target interval. We instead compared valid trials with the baseline to unveil the brain regions and their timings of activation subserving deployment and maintenance of visuospatial attention after the target onset. Our findings show an overarching involvement of dorso-parietal and visual areas in voluntary orienting of attention, confirming the role played by the DAN and occipital regions in managing this process (Ptak & Schneider, 2010). Particularly, a bilateral SPL and an extra-striate engagement have been highlighted both during the cue-target interval and after the target onset. Our cue-related results are in agreement with previous studies employing spatial cueing paradigms. Mayrhofer and colleagues (2019) explored anticipatory pre-target activity linked to the informative cue, suggesting a correlation between activations in brain regions overlapping with our bilateral SPL ROIs and selective attentional behavioral effects on task performance. In addition, Vandenberghe and colleagues (2012) revised structural lesion studies investigating the role of the superior parietal cortex in spatial attentional disorders which supported an involvement of SPL in cue-related attentional shifting independently from the cued direction. Concerning extra-striate areas, our EROS results reveal a solid activation of cuneus, whose contribution is also supported by our GCA performed on after-cue-onset data. Indeed, cuneus has been found to predict ISPL activity at a different time lag, pointing out a dorso-visual predictive interaction underlying intentional deployment of visuospatial attention after the presentation of an informative cue. This statement is in line with prior evidence indicating both that early activations of extra-striate cortices account for endogenously orienting and the contribution of SPL in triggering a shift of attention, especially when it is decoupled from central fixation (Kelley et al., 2008; Rihs et al., 2009). The critical involvement of cuneus and SPL has been uncovered after target onset as well. These findings are totally in accordance with the results highlighted in Parisi et al. (2020), where cuneus and SPL were the main outcomes of EROS after-target-onset analyses obtained from a discrimination spatial cueing task. As to Granger results, they seem to bring out a dorso-visual mutually predictive interplay also over this time window, further supporting the crucial role of dorso-parietal nodes of the DAN (i.e., SPL) and extra-striate regions (i.e., cuneus) in a top-down attentional information flow (Doesburg et al., 2016; Proskovec et al., 2018). Moreover,

previous fMRI (Bressler et al., 2008; Lauritzen et al., 2009) and EROS findings (Parisi et al., 2020) by exploring the connectivity between visual and dorso-parietal areas unfolded the implication of IPS and early visual regions during sustained attention. Our Granger results are in line with these pieces of evidence, showing the coming into play of V1 and IPS in a dorso-visual reciprocally predictive interface. Indeed, these regions, especially IPS, have been revealed to be implicated in top-down control attentional mechanisms by representing sustained states of peripheral attention (Kelley et al., 2008; Parisi et al., 2020).

Our orienting analyses also exhibit seemingly uncommon findings, i.e., the involvement of the VAN in covertly orienting visuospatial attention. Specifically, ITPJ and rTPJ have been shown to be engaged in performing an attentional orienting process after the cue onset and after the target onset, respectively. Nevertheless, concerning the contribution of ITPJ, consolidated by both our EROS and Granger results, recent fMRI studies support this evidence by highlighting ITPJ activations in spatial attentional tasks (Doricchi et al., 2010; Wisniewski et al., 2015; Abrahamse & Silvetti, 2016). In particular, DiQuattro and Geng (2011), by availing of a visual search paradigm, demonstrated the role of ITPJ in detecting informative salient aspects and using them to initiate endogenous and effective attentional orienting.

More infrequent could appear the directed influence observed from IIPS to rTPJ after the target onset, which represents a brain region typically active during reorienting attention from an attended to an unattended location. We believe that this result could not have a specific contribution to the orienting process, given that it emerges in GCA only, and does not predict, in turn, any other ROIs, thus likely not contributing to carrying on the attentional stream. However, a TMS-fMRI study conducted by Leitão and colleagues (2015) by administering a sustained spatial attention paradigm, which did not include reorienting mechanisms, highlighted the importance of IPS for modulating neural processes in the rTPJ. Further research is, thus, needed to ascertain a possible contribution of rTPJ in orienting processes.

To summarize, our results suggest a predictive pattern between dorsal and visual regions that persists in both the analyzed functional contrasts, lasting over the whole orienting process, from the cue occurrence until after the target onset. This dorsal

and visual network, whose main components are bilateral SPL and the dorsal portion of the cuneus, is responsible for each neural step of endogenous attentional orienting. Moreover, our findings exhibit pretty new evidence of the engagement of bilateral ventral network in this cognitive mechanism.

4.2 Reorienting

In the present work, the contrast between invalid trials and the baseline was also considered with the purpose of examining visuospatial attentional reorienting. Indeed, comparing invalid trials with the baseline allowed us to segregate the brain regions activated by targets occurring at an uncued location after an endogenous attentional expectation generated by the cue. Our results point out a clear implication of bilateral dorso-parietal regions along with visual areas in processing invalid trials considering an after-target onset time window. This evidence is in keeping with previous studies supporting the involvement of the DAN in reorienting attention toward unexpected target locations (Doricchi et al., 2010; Vossel et al., 2009, 2012). More precisely, we observed bilateral recruitment of IPS while the importance of ISPL emerged again. As we stated above, invalid trials usually yield specific sub-mechanisms, such as perceiving a mismatch between expectations and reality, disengaging, shifting, and re-engaging attention from the cued location to the correct one. These cognitive stages appear underpinned by the aforementioned dorso-parietal regions differently, as suggested by Spadone and colleagues (2021): SPL was found to be entailed by shifting and reorienting attention processes, while IPS is entailed by sustaining attention processes. This last evidence seems to be in line with our current EROS results, but to better understand how these brain regions interact to accomplish their roles, we further analyzed data by applying GCA. Surprisingly, our invalid versus baseline contrast did not bring out any significant contribution of the ventral network, in particular of rTPJ, in endogenous reorienting processes. Again, GCA helped us expand our functional results and better comprehend the predictive relationships among dorso-parietal, ventral, and visual areas during reorientation of attention after encoding the discrepancy between cue-related expectancy and the actual event. At first general sight, predictive connections are several more than

those involved in the orienting process. In the very beginning, we noticed an early predictive interface among the same cortical regions (i.e., dorso-parietal areas predicted dorso-parietal areas and visual areas predicted visual areas), followed by a dorso-visual stream in which dorso-parietal (bilateral SPL and bilateral IPS) and visual areas (V1 and cuneus) reciprocally predict each other in a post-target time window ranging between 200 and 600 ms. In addition, these data show the coming into play of the ventral network, embodied by rTPJ. The activity of rTPJ is actually influenced by both dorso-parietal (i.e., rSPL and rIPS) and visual regions (i.e., cuneus) at later timeframes after the target onset, highlighting a recurrent predictive pattern. Indeed, rTPJ exerts, in turn, predictive effects on both visual and dorso-parietal regions, subsequently in time.

Overall, our reorienting results are partially in accordance with the already cited MEG study by Proskovec and colleagues (2018). Investigating attentional reorienting in a visuospatial Posner-like task, authors found greater functional connectivity in the alpha band across bilateral SPL, highlighting a significant contribution of this region in serving control-related attentional processes. Similarly, we reported in EROS and GCA results, respectively, stronger activations and predictive relationships between bilateral SPL, which is thus fundamental in controlling and shifting attention during invalid trials. However, Proskovec and colleagues (2018) suggested the disengagement of attention from the cued incorrect location to be managed by the VAN, more precisely by the right IFG, which revealed increased theta activity during early processing of invalid targets. This interpretation does not fit with our results, which, instead, seem to indicate that disengaging attention from the invalidly cued location and shifting and re-engaging it to the uncued location are subserved by a persistent and mutually predictive dialogue among dorso-parietal and visual regions. Furthermore, rTPJ, which in our study is the primary representing node of the VAN and whose contribution is disclosed mainly by means of GCA, seems not to participate in this triggering and reorienting process by being predicted later in time and unveiling the timing of activations typical of P3b (300-500 ms post-target). This evidence enables us, on one side, to discard the idea of the VAN as a “circuit-breaker” or a trigger of the

reorienting process and, on the other side, to support the “Contextual Updating” hypothesis (Geng & Vossel, 2013; Polich, 2007), sustaining a post-perceptual and supervision connotation of the role of rTPJ. This supervision should be fulfilled by constantly updating internal models of the behavioral context (Doricchi et al., 2022). More precisely, rTPJ should be responsible for updating the probabilistic cue-target contingencies in a trial-by-trial manner in order to preserve or change the attentional task set (Doricchi et al., 2010). This monitoring function seems to be more relevant when invalid trials occur. Due to their unexpected nature, they would generate a stronger need to update the internal model about the cue-target association, in order to perform accurately in subsequent trials. Nevertheless, it has been demonstrated that valid trials also yield a post-perceptual updating mechanism (Arjona Valladares et al., 2017). This evidence would be in accordance with our GCA-orienting findings, highlighting the prediction of activity in rTPJ carried out by dorso-parietal regions. We can speculate that the difference between valid and invalid trials in the strength of engendering an updating process could be supported by our results: rTPJ activity predicted during valid trials does not further continue the flow of information, while rTPJ activity predicted during invalid trials exerts in turn directed influences on, later in time, DAN and visual regions, unfolding a strengthened procedure of integrating novel information with the preexisting internal model.

With respect to the absence of significant activity of rTPJ in invalid versus baseline EROS contrast, we believe this could be due to the specific paradigm we employed. Our location-cueing paradigm was purposely implemented to investigate the spatiotemporal dynamics of orienting and reorienting processes requiring a low cognitive demand. At a behavioral level, these neural mechanisms are embodied by both the validity effect and the contextual updating effect. The validity effect is a general, really strong effect, globally and uniformly distributed over the whole task performance. Therefore, its robustness and global nature likely prevented it from being influenced by the current low cognitive load request. On the other hand, the contextual updating process is an effect, more particularly distributed than the validity effect, and more dependent on specific manipulations of the employed paradigm, which could thus had been impacted by the low cognitive load request.

Consequently, we supposed the updating process has been prevented from being detected by EROS analyses, probably overwhelmed by the stronger and more overarching validity effect. This apparent issue has been easily overcome by applying GCA to EROS functional data, letting us observe the neural behavior of rTPJ during visuospatial attentional events with a high level of reliability.

5. CONCLUSIONS

The present study intended to disclose the functional interplays among the cortical areas corresponding to the posterior nodes of the DAN and the VAN, underlying covert endogenous orienting and reorienting processes evoked through a detection Posner-like paradigm. Taken together, our findings are in keeping with Parisi et al. (2020), supporting the role of a dorso-visual network in controlling, directing, and re-directing visuospatial attention in both orienting and reorienting mechanisms. Regarding the contribution of rTPJ, both studies suggest a post-perceptual role in updating the internal model of the cue-target relationship as a function of new information on a trial-by-trial basis. Finally, the current study discloses a quite robust implication of the ITPJ in the cue-target orienting procedure. To conclude, our evidence confirms and expands the current literature by demonstrating the likely neural underpinnings of top-down control and updating attentional mechanisms. However, despite the novelty and the scientific contribution of this study, it was not without limitations. The main one was the impossibility of covering frontal areas by means of our EROS montages, preventing us from investigating the activity of FEF and VFC, which are known to have a fundamental involvement in visuospatial attentional processes (Proskovec et al., 2018; Spadone et al., 2021; Vossel et al., 2012). Therefore, further EROS studies should try to include frontal regions in functional analyses to examine how they take part in the predictive visual, dorso-parietal and ventral relationships engaged by endogenous attention. Lastly, this study lacks behavioral and especially functional analyses examining the effect of the side (right or left) of the stimuli, which might induce consequent brain activations after both the cue and the target onset. These analyses have not been performed due to the number of right and left trials, which would have been too small to tackle the low signal-to-noise ratio typical of the EROS

technique. Therefore, further studies should include an adequate number of trials to investigate the potential effects of the stimulus side on DAN, VAN and visual areas patterns of activations.

EXPERIMENT 2

1. INTRODUCTION

The right temporoparietal junction (rTPJ) is a human brain region comprising the ventral nodes of the right parietal cortex, namely the Supramarginal and Angular gyri, together with the right caudal portion of the Superior Temporal Gyrus contiguous to the posterior ending of the Sylvian fissure (Doricchi et al., 2022). In the last two decades, much effort has been made to identify the exact nature of its role in supporting human cognition without attaining a collectively shared interpretation. This issue has been fostered by evidence suggesting both the involvement of rTPJ in multiple cognitive processes and its parcellation in anatomically different subregions (Caspers et al., 2006). Indeed, it is still unclear whether these subsectors mediate distinct domain-specific functions, as stated by the “Fractionation view” (Krall et al., 2015; Scholz et al., 2009), which associates distinguishable rTPJ subregions with specific cognitive functions, or, alternatively, rTPJ underpins one common cognitive mechanism across distinct cognitive domains (Doricchi et al., 2022). The latter perspective, known as the “Overarching view” (Schuwerk et al., 2017, 2021), suggests a unifying overarching role of rTPJ in monitoring surrounding contingencies. More specifically, this brain region has been linked to the more general function of “Contextual Updating” (Geng & Vossel, 2013), which refers to the ability to update internal models of the current behavioral context to build expectations and responses accurately.

Despite the still-existing debate, rTPJ engagement in the visuospatial attention domain is widely accepted (Dugué et al., 2018), recognizing it as a critical hub of the Ventral Attentional Network (VAN), whose activity is, in turn, associated with endogenous reorienting of attention toward unexpected but behaviorally relevant visual stimuli (Corbetta et al., 2008). Initially, rTPJ was thought to contribute to the reorienting process by interrupting the top-down deployment of attention performed by dorso-parietal regions (i.e., the cortical regions included in the Dorsal Attention Network, DAN) and successively allowing the same cortical nodes to proceed with reorienting attention toward unexpected but task-relevant stimuli, thus playing the role of a sort of “circuit-breaker” (Corbetta & Shulman, 2002). This perspective

would entail an early recruitment of rTPJ during visuospatial attentional processes. Nevertheless, the opposite situation has been shown more recently, revealing a later attentional engagement of rTPJ occurring in a time window ranging from 400 to 500 ms after the target onset (Parisi et al., 2020). This evidence is in line with the association between the rTPJ and the P3b (Polich, 2007). The latter, indeed, represents a sub-component of the electrophysiological potential P300, usually occurring in a late post-target time window (300-500 ms). Moreover, P3b is traditionally considered a neurophysiological correlate of contextual updating (Arjona & Gómez, 2013; Donchin & Coles, 1998; Polich, 2007), which, in the visuospatial attentional framework, should arise after endogenously reorienting attention toward unattended target locations (Mengotti et al., 2017). Accordingly, rTPJ should contribute to visuospatial attentional processes by updating internal models of the attentional context in order to create expectations and properly guide future actions (Doricchi et al., 2010; Parisi et al., 2020). It appears evident that there is no unequivocal consensus, even concerning the contribution of rTPJ to the attentional sphere, remaining unclear whether it is responsible for visuospatial endogenous reorienting or contextual updating.

The purpose of the current study is to elucidate the role of rTPJ in visuospatial attentional processes by employing a behavioral task where reorienting and contextual updating can be separately investigated. Modified versions of the classical location-cueing paradigm (Posner, 1980) can address this issue. The visuospatial adaptation of this paradigm is usually characterized by a central predictive cue that may (valid trial) or not (invalid trial) predict the location of an impending visual target (Capotosto et al., 2012; Natale et al., 2009; Vossel et al., 2006). The deployment of attention to one target location improves, in terms of Reaction Times (RTs), the efficiency of responding to the target on that side while worsening it on the other side, reflecting the so-called “Validity Effect”. This effect results from the advantage of being attentionally oriented to the cued location and the cost produced by redirecting attentional resources from the location indicated by the cue to the uncued one (Posner, 1980). Furthermore, it has been shown that participants performing location-cueing paradigms execute a cognitive assessment

concerning the validity/invalidity of the current trial, causing behavioral effects that are transferred to the subsequent trial (Gómez et al., 2009). Specifically, faster RTs emerge when valid trials are preceded by valid trials (VV) compared to when valid trials are preceded by invalid ones (IV). Likewise, a benefit in RTs emerges when invalid trials are preceded by invalid trials (II) compared to when invalid trials are preceded by valid trials (VI). These behavioral mechanisms represent the so-called Intertrial (Validity/Invalidity) effect, which can be thus described by the following behavioral pattern concerning the RTs linked to the second trial of each 2-trial sequence: $VV < IV < II < VI$ (Arjona & Gómez, 2011). Examining the Validity Effect and the Intertrial Effect provides the possibility to segregate the endogenous reorienting and the contextual updating, respectively. In particular, the Validity Effect, representing an index of the time needed to disengage and shift attention from the attended to the unattended location and depending on the global predictive value of cues, stands for a clear outcome of endogenously reorienting attention toward the unexpected but behaviorally relevant target location. Meanwhile, the Intertrial Effect reflects the influence that the assessment of the validity condition in one particular trial (n-1) has on the performance of the following trial (n). It thus constitutes a tangible indicator of a dynamic updating of the cue-target conditional probabilities on a trial-by-trial basis (Arjona Valladares et al., 2017). Indeed, the credibility conferred to the cue changes with each trial, making the strength in deploying attention to the cued location higher or lower. Hence, in order to shed light on the precise role of rTPJ in visuospatial attentional processes, we employed a non-invasive neurostimulation technique, i.e., the Transcranial Magnetic Stimulation (TMS), during the administration of a location-cueing paradigm. It is well known that online TMS (i.e., administered simultaneously with the execution of the behavioral task) interferes with the neural activity of a definite cortical region with a spatial resolution of the order of millimeters (Schuwerk et al., 2021) and good temporal precision. Applying TMS over rTPJ within a specific time window enabled us to directly assess the involvement of rTPJ in visuospatial attentional dynamics. These processes would be induced by means of a visuospatial version of a location-cueing task requiring both directing attention according to the global meaning of the cue and updating the cue-target trialwise contingencies in order to

perform accurately. Therefore, any effect on the participants' task performance resulting from the interference of TMS would be informative on the rTPJ's role in attentional reorienting and contextual updating. More specifically, we hypothesized that a potential reduction of the Validity effect after rTPJ TMS stimulation would be an index about the rTPJ's role in managing attentional reorienting, whereas we predicted that a possible decrease of the Intertrial effect after rTPJ TMS stimulation would indicate rTPJ involvement in contextual updating processes within an attentional perspective.

2. MATERIALS AND METHODS

2.1 Participants

Nineteen right-handed (as assessed by the Edinburgh Handedness Inventory, Oldfield, 1971) adults (4 males) were recruited for the study. Their ages ranged between 20 and 30 years (mean age \pm standard deviation: 24.8 ± 3.4), and they had normal or corrected-to-normal vision. Written informed consent was obtained from each volunteer in accordance with the principles laid down by the Declaration of Helsinki. The experimental protocol has been approved by the local Ethics Committee. As assessed by a safety screening questionnaire (adapted from Rossi et al., 2009), all participants were negative for the risk factors associated with TMS: none reported any history of epilepsy or migraine, cardiac pacemaker, neurological disorders, current treatment with any psychoactive medication and pregnancy. Thirteen participants received reimbursement for their participation, while six participants were internship students from the University of Verona. All but one (author E.C.) participants were naïve to the aims of the study.

2.2. Experimental procedure

In a within-subject design, participants underwent two experimental sessions over two days. In each experimental session, both active TMS and sham stimulation were delivered and interspersed by a 20-minute break, independently from the starting stimulation, which was counterbalanced across participants. Moreover, the

order of active TMS and sham stimulations was alternated between the two experimental sessions for each participant.

2.3. Behavioral Task

Participants were individually tested in a dimly lit testing room. During each experimental session, they sat in front of a 24-in. LCD monitor (resolution 1920x1080, refresh rate of 144 Hz) at a viewing distance of 57 cm. They leaned on a chinrest with forehead support so that their eyes could be adjusted to the center of the screen and head movements could be restricted when TMS was positioned.

The same behavioral task of Experiment 1 (See **2.3 Behavioral task**) was administered, with some crucial changes. Indeed, a location-cueing paradigm with central cueing was employed (Posner, 1980). Stimuli were generated using E-Prime 2.0 software (E-Prime Psychology Software Tools Inc., Pittsburgh, PA, USA) and consisted of vertical or horizontal, black-and-white, 2° square gratings. Participants were asked to maintain fixation on a centrally presented black point lasting for 500 ms on a grey background. Afterward, a central predictive cue (i.e., an arrow) was shown above the fixation point (duration 200 ms). After a random interval ranging from 400 to 600 ms, the target was presented for 150 ms at an eccentricity of 2° from the fixation point to the inner edge along the horizontal meridian. The intertrial interval was random, ranging from 3900 to 4000 ms. Participants were asked to pay attention to the side indicated by the cue and discriminate the target's orientation as fast as possible by pressing the “b” button with their right index finger or the “n” button with their right middle finger on a QWERTY IT keyboard. Instructions were counterbalanced across participants: “b” had to be pressed when vertical targets appeared, “n” had to be pressed when horizontal targets appeared, and vice-versa. Horizontal and vertical trials randomly occurred in each block with the same probability. Likewise, left and right targets were equally distributed within a single block, appearing in a random fashion. Each experimental session was divided into ten blocks, for a total of 20 blocks per participant. The percentage of cue validity (%CV) was fixed so that in each block, 75% of trials were valid, that is, when the cue gave the correct indication about the impending target location, and 25% of trials were invalid, that is when the target appeared on the unattended side.

Importantly, the cue direction was kept constant throughout a block: in half of the blocks ($n = 10$), it pointed to the right, while in the other half, it pointed to the left visual hemifield. Participants were informed that the location indicated by the cue had a higher probability of including the target while unaware of the exact CV%. Moreover, given the importance of trial history in influencing RTs performances, four 2-trial sequences were considered in building and programming the experiment in order to assess the impact of the previous trial (i.e., trial $n-1$) on the following one (i.e., trial n). These sequences were valid trial-valid trial (VV), invalid trial-valid trial (IV), invalid trial-invalid trial (II), and valid trial-invalid trial (VI). All sequences were included in each block in a pseudo-random order, aiming to obtain at least 60 presentations for each sequence within the whole task (see Table 1 for the exact number of presentations of each sequence per block). Each participant was presented with the same sequence of trials in each block, which consisted of 39 valid trials and 13 invalid trials, for a total of 1040 trials (780 valid, 260 invalid) per participant. In each experimental session, active TMS and sham stimulation were administered for five consecutive blocks, respectively, for a total of 10 active blocks and 10 sham blocks per participant. Accordingly, block order, which was random during the first experimental sessions, remained unchanged for each participant over the second experimental sessions.

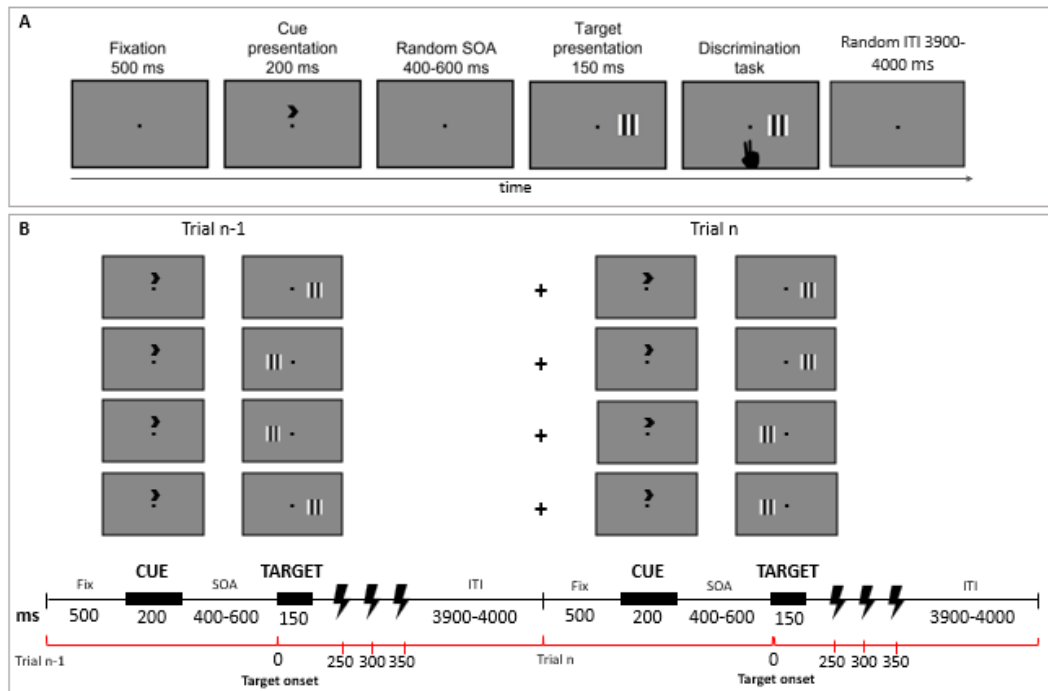


Figure 1. Experimental Paradigm

(A) Timeline of the experimental paradigm for a right validly cued trial. A fixation point was presented for 500 ms followed by a central predictive cue lasting 200 ms. After a random interval ranging from 400 to 600 ms, the visual target was presented for 150 ms. Participants had to discriminate the target orientation (i.e., vertically or horizontally oriented gratings) within an intertrial interval ranging from 3900 and 4000 ms. (B) The four types of considered 2-trial sequences are shown, together with the temporal sequence of events of trial n-1 and trial n (reported in the inferior part of the figure). The sequences are ordered as follows: VV, IV, II, VI. rTMS pulses were delivered in every trial at 250, 300, and 350 ms after the target onset.

Table 1. Number of presentations of each sequence per block

Block\Sequence	VV	IV	II	VI
Block 1	31	7	7	6
Block 2	32	6	7	6
Block 3	31	7	6	7
Block 4	31	7	6	7
Block 5	32	6	7	6
Block 6	31	7	7	6
Block 7	32	6	7	6
Block 8	31	7	6	7
Block 9	31	7	6	7
Block 10	32	6	7	6

2.4 TMS protocol

Triple-pulse magnetic stimulation was delivered over rTPJ through a 70 mm figure-of-eight coil connected with a Magstim Rapid2 system (Magstim Company Limited, Whitland, UK). The TMS coil was held tangentially to the scalp, with the handle pointing backward. Three pulses at 20 Hz per trial were administered starting from 250 ms after the target onset. The TMS pulse triggers were computer-

controlled via the same script of the behavioral task. Stimulation intensity was set to 100% of each participant's resting motor threshold (rMT) derived from the left primary motor cortex activating the right first dorsal interosseous (FDI) muscle. The rMT was the lowest stimulus intensity that elicits five of ten motor-evoked potentials with an amplitude of at least 50 μ V recorded through BrainAmp amplifiers (Brain Products GmbH, Munich, Germany– Brain Vision Recorder) and four Ag/AgCl electrodes. Consequently, the mean stimulation intensity across participants was $58 \pm 6\%$ (mean \pm SD).

A neuronavigation software (SofTaxis, E.M.S., Bologna, Italy) combined with a 3D optical digitizer (Polaris Vicra, NDI, Waterloo, Canada) was used throughout the whole experimental session to guide and constantly monitor the TMS-coil placement with an accuracy of 2 mm. Moreover, 12 participants out of 24 underwent a T1 magnetic resonance imaging (MRI) scan prior to this experiment, providing the possibility of implementing T1-weighted images into the neuronavigation system. As a result, rTPJ (i.e., the stimulation site) coordinates were chosen individually for each of these participants by visually checking the anatomical localization of rTPJ (i.e., in the posterior part of the right temporal gyrus) in each participant's brain and adjusting them according to the rTPJ coordinates employed by Mengotti et al. (2017). For those participants whose structural MRI was not available, an estimated MR-based head model was individually created using the neuronavigation software and the same procedure explained in the first experiment of this thesis (See **2.4 Optical recording**). The rTPJ coordinates utilized for the second half of the sample consisted of the mean rTPJ coordinates from the first 12 participants (i.e., $x=66$, $y=-41$, $z=18$)

A 70 mm figure-of-eight placebo coil (Magstim Company Limited, Whitland, UK) was employed for the control sham stimulation, appearing identical to the regular coil. The sham coil was held tangentially to the surface of the scalp over rTPJ in order to mimic the placement, the noise, and the mechanical vibration of TMS without actually stimulating the brain tissue. Participants were provided with commercial earplugs to protect them from the machine's noise (Rossi et al., 2009) during both active and sham stimulation and to prevent responses from being influenced by the intensity of the coil click.

2.5. Behavioral data analysis

Data were processed using E-Prime 2.0 software and analyzed with Statistica, version 8. For each participant, horizontal and vertical trials were systematically collapsed. Mean reaction times (RTs) and the corresponding standard deviations (SDs) were computed for each stimulation condition (Active and Sham), each validity condition (valid and invalid, independently from cue and target side), and each sequence (VV, IV, II, VI) across participants. Trials with RTs exceeding ± 3 SDs from the mean in each condition were considered outliers and removed from the analyses. Subsequently, RTs were entered in a repeated measures analysis of variance (ANOVA) with stimulation and validity conditions as within-subject factors. Furthermore, a second repeated measures ANOVA with stimulation and sequence conditions as within-subject factors was conducted by analyzing RTs related to the second trial of each 2-trial sequence. Where needed, Bonferroni-corrected post-hoc t-tests were applied.

3. RESULTS

The repeated-measure ANOVA conducted on mean RTs, considering stimulation and validity as within-subject factors, revealed a significant main effect of the validity condition ($F_{(1,18)} = 44.959$, $p < 0.001$, $\eta^2_p = 0.714$), highlighting faster RTs in valid (469 ms) compared to invalid trials (492 ms). Importantly, neither the stimulation condition nor the interaction effect reached statistical significance ($F_{(1,18)} = 0.0657$, $p = 0.801$, $\eta^2_p = 0.004$); $F_{(1,18)} = 0.174$, $p = 0.682$, $\eta^2_p = 0.01$). This result suggests an intact Validity Effect in both Active and Sham stimulations.

As to the repeated-measure ANOVA that took into account stimulation and sequence conditions as within-subject factors, executed on mean RTs related to the second trial of each 2-trial sequence, it indicated a significant main effect of sequence ($F_{(1,18)} = 29.852$, $p < 0.001$, $\eta^2_p = 0.624$). In contrast, no significant difference in stimulation conditions was found ($F_{(1,18)} = 0.051$, $p = 0.823$, $\eta^2_p = 0.003$). Notably, the interaction between stimulation and sequence reached statistical significance ($F_{(1,18)} = 2.884$, $p = 0.044$, $\eta^2_p = 0.138$). Hence, to further investigate this effect, Bonferroni-corrected post-hoc t-tests were carried out,

revealing a crucial difference between Active and Sham conditions, as the following: RTs of the last two sequences, II and VI, showed to be significantly different in the Sham ($p = 0.015$), while their difference did not reach statistical significance in the Active condition ($p = 1.000$).

Overall, these results suggest an intact attentional orienting benefit in target discrimination in valid trials, along with an intact cost of rearranging attentional resources in invalid trials, suggesting that rTPJ contribution in reorienting attention toward unexpected locations is not fully tenable. Unlike, the Active TMS stimulation seems to have impacted the inter-trial effect, severely reducing the difference between II and VI. This evidence represents a key behavioral outcome linked to the attentional context updating on a trial-by-trial basis.

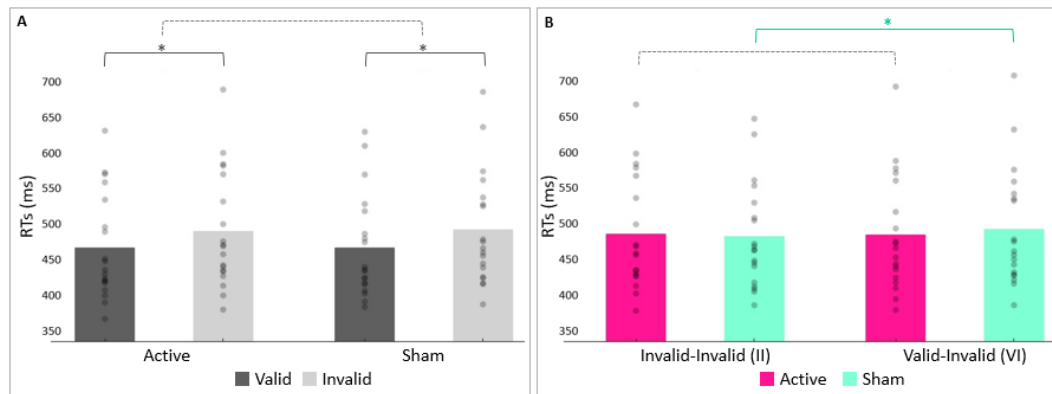


Figure 2. Behavioral results.

(A) Validity effect results. Mean response times are plotted as a function of both validity and stimulation conditions. Error bars represent standard errors. Significant and non-significant effects are shown, these last via a dashed line. (B) Intertrial effect results considering II and VI only. Mean response times are plotted as a function of both sequence and stimulation conditions. Significant and non-significant effects are shown, these last via a dashed line. For each condition of each graph, individual data are plotted (grey dots) along with averaged values.

4. DISCUSSION

The goal of the present study was to clarify the involvement of rTPJ in visuospatial attentional processes by combining behavioral measures and online rTMS. Refining the knowledge around rTPJ functioning constitutes a remarkable matter due to its widely known implication in a considerable number of cognitive processes and the ensuing cognitive and neuropsychological disorders, such as spatial neglect, which is strictly related to attentional mechanisms. Spatial neglect is primarily described as a deficit in spontaneously reorienting attention to stimuli occurring in the

contralateral visual field after damage mainly to the right inferior parietal cortex (De Schotten et al., 2005; Mort et al., 2003; Posner et al., 1984) usually encompassing rTPJ. These pieces of evidence share conclusions with a large number of fMRI studies revealing stronger rTPJ activation in response to invalidly cued targets (i.e., targets appearing in one unattended spatial location that is rather relevant for the behavioral task), accordingly ascribing to it a specific role in triggering attentional reorienting toward unexpected locations (Doricchi et al., 2010; Indovina & MacAluso, 2007; Natale et al., 2010; Vossel et al., 2006). Therefore, both neuroimaging and neuropsychological findings supported the involvement of rTPJ in attentional reorienting by communicating early in time with dorsal regions through frontal areas. However, more recently, it has been argued that this model could not be totally accurate, considering that more precise tools in identifying the timings of activation of cortical brain regions (for instance, TMS) have highlighted a later rTPJ recruitment (Geng & Vossel, 2013).

Based on these premises, our study has been developed with the purpose of exploiting rTMS high temporal resolution, along with its likewise good spatial localization power, in order to temporarily interfere with rTPJ activity at predefined timings. Accordingly, we were allowed to observe direct behavioral consequences. These latter were unveiled through a location-cueing paradigm capable of disregarding two essential behavioral effects: the validity effect, representing the implementation of the attentional reorienting process, and the inter-trial validity effect, revealing the ability to update one's internal model about the predictive value of the spatial cue. Thereby, on the basis of the likely different impact of rTMS over rTPJ on the two behavioral outcomes, we could attribute to rTPJ a functional role either in reorienting visuospatial attention towards unattended but relevant locations or in updating the internal representations of cue-target predictions in a trial-by-trial manner.

Our findings seem to suggest a clear implication of rTPJ in this second option. The attentional benefit deriving from valid trials, together with the attentional cost in responding to unattended targets, depicted by slower RTs in invalid trials, emerged to be unaltered by the action of the rTMS. Comparable validity effects have indeed been found between the rTMS and the Sham conditions, letting us conclude that

triggering the reorientation of attention towards uncued but behaviorally relevant spatial locations should not be subserved by rTPJ.

In contrast, TMS interference over rTPJ seems to have an impact on the efficacy of participants' predictions in a given trial in prompting changes in the processing of the subsequent trial. In other words, rTMS affected the interaction between the validity of the previous trial and the validity of the current trial, which appears to be intact after a Sham stimulation. More specifically, interesting results have been found examining invalid trials: while greater costs in RTs were discovered when an invalid trial was preceded by a valid trial rather than an invalid one, in the Sham condition, this difference was not detected in the rTMS condition, representing the direct behavioral consequences of TMS application. The disturbance of these last two sequences solely (i.e., II and VI), carried out by interfering with rTPJ activity, is supported by the existing literature: rTPJ activation is usually elicited by invalid trials (Natale et al., 2010) and more strongly when the cue validity is high (Vossel et al., 2006), as in our study (i.e., 75%), namely when the violation of expectations is more robust. Moreover, the nature of the behavioral paradigm used in this study to separately inspect attentional reorienting and updating needs to be taken into account. Mainly, the cognitive effort required to discriminate the orientation of the stimuli was relatively low, leading the two behavioral effects considered (i.e., the validity effect and the Intertrial effect) to emerge differently. More precisely, the validity effect consists of a general and robust effect, consistently distributed over the whole task performance, mainly representing the reorienting process. On the other hand, the Intertrial effect is more specifically distributed than the validity effect and more dependent on specific manipulations of the behavioral paradigm, letting us believe that here a match between one's expectation and reality was not enough to elicit a detectable need to update future predictions in order to behave appropriately. Hence, we speculate that rTMS could not efficiently interfere with the contextual updating process associated with valid trials because of its too modest fulfillment. In contrast, a mismatch between one's expectations and reality was followed to a greater extent by the need to update mental models to behave appropriately, enlightening a plausible explanation for the TMS-related disruption of behavioral outcomes linked to invalid trials only.

Besides being in accordance with studies including rTPJ functioning within the contextual updating framework (Doricchi et al., 2010, 2022; Geng & Vossel, 2013; Mengotti et al., 2017; Parisi et al., 2020), our findings are in keeping with a variety of ERP studies (Arjona et al., 2014, 2018; Arjona & Gómez, 2013; Arjona Valladares et al., 2017; Gómez et al., 2009, 2019) investigating ERPs components to track the time-course of events in Central Cue Posner Paradigms, where performances on specific trials highly depend on the performance of the previous ones. In particular, by grouping trials into 2-trial sequences, Arjona and colleagues (2014) analyzed P3b data, whose time window perfectly fits our TMS pulse timings, pointing out higher amplitude in the VI sequence than in the II sequence. Hence, the agreement between our results and the ERP data mentioned above could further confirm the association between P3b and rTPJ, letting us ultimately assign to it a role in updating trialwise predictions about cue-target relationships in a location cueing paradigm. Our conclusions are additionally corroborated by the fact that the contextual updating framework also stands for a reasonable account to explain rTPJ involvement in many other domains, such as the theory of mind and body awareness (Blanke et al., 2005; Decety & Lamm, 2007). Indeed, they similarly involve stimulus-triggered event updating of previous information with new upcoming events provided by the external environment or person or internal body signals (Geng & Vossel, 2013; Mengotti et al., 2017) necessary to predict future contingencies related to the specific cognitive process.

5. CONCLUSIONS

In the current study, we applied online rTMS with the intention of investigating the role of rTPJ in visuospatial attentional mechanisms directly. Taken together, our data disclosed that interfering with rTPJ activity from 250 to 350 ms after the target onset throughout the administration of a location-cueing paradigm selectively affected participants' updating of the predictive value assigned to the spatial cue, trial-by-trial, leaving intact the ability to reorient attention towards uncued behaviorally relevant spatial locations.

However, despite the novel insights provided by the current study into the understanding concerning rTPJ functioning and even that our paradigm is based on previous findings related to rTPJ timings of activation, this study could be limited by the lack of stimulation at early timeframes. More precisely, without interfering with rTPJ functioning at early stages after the target onset, we could not definitely rule out the possibility that rTPJ would be engaged in reorienting mechanisms as well, typically found to occur relatively early in time. Therefore, further TMS studies should try to interfere with rTPJ activity at both early and late time windows in order to disregard rTPJ involvement in triggering the attentional reorienting process. Eventually, given the ever-growing relevance of left TPJ in both attentional reorienting and post-perceptual mechanisms, interesting studies could be additionally conducted to compare TMS-related consequences after the stimulation of both rTPJ and lTPJ.

EXPERIMENT 3

This experiment was carried out at the Institute of Neuroscience and Medicine (INM-3, Forschungszentrum Jülich) under the supervision of Professor Simone Vossel.

1. INTRODUCTION

The human brain has to deal with a constantly evolving environment, which is typically characterized by continuous uncertainty about stimuli and outcomes. The attentional system is involved in a persistent evaluation of the surroundings in an attempt to cope with this uncertainty by filtering the most relevant contextual stimuli and guiding subsequent actions adaptively (Arjona et al., 2014). In order to accomplish this function, attentional mechanisms provide a continuous assessment of the environment based on present goals and past experience (Friston & Kiebel, 2009). In other words, the attentional system tries to predict the likelihood of the occurrence of events on the basis of one's internal representations or internal mental models of statistical regularities, which, in turn, result from previous experience (Arjona & Gómez, 2013). Internal models stand as a valuable tool to optimize forthcoming performances when they are both sufficiently accurate in representing regularities and sufficiently flexible to be updated when contingencies change and current predictions are no longer appropriate (Go et al., 2022). The utilization of an accurate internal model entails well-predicted events, namely ones with a high probability of occurrence according to the model, and surprising events, namely ones detaining a low probability of occurrence according to the model (O'Reilly et al., 2013). These latter can challenge the internal model by contradicting expected outcomes. At this point, surprising events can be considered as either random noise (leaving the internal model unchanged) or warnings that the environment has changed (leading to model updates) (Filipowicz et al., 2018). This dynamic adjustment, which continually influences decisions in situations of uncertainty, is a key component of a well-known behavioral paradigm, the location-cueing Posner task (Posner, 1980). This task is characterized by a central spatial cue providing relevant probabilistic information about the location of an upcoming visual target.

This information is correct in most trials (in which the upcoming target is presented at the cued location, so-called valid trials), while, in a lower proportion of trials, the cue gives a wrong indication as the target is presented at an uncued location (invalid trials). Valid and invalid trials thereby represent high probability occurrence and low probability occurrence outcomes, respectively, and a behavioral consequence is that attention is oriented to the cued location, causing Reactions Times (RTs) to the targets to be faster in valid than invalid trials. Accordingly, it has been demonstrated that attentional processes are critically affected by trial history and the current probabilistic context (Vossel et al., 2015). For instance, both RT advantages for valid trials and RT costs for invalid trials are larger after a valid than an invalid trial (Arjona & Gómez, 2011). Importantly, the RTs difference between invalid and valid trials, which is called “Validity Effect” (VE) and represents the time needed to disengage and shift attention from the cued to the uncued, behaviorally relevant location, depends on the percentage of cue validity (%CV), that is, the proportion of validly versus invalidly cued trials. A higher %CV is associated with a higher VE (Vossel, Mathys, et al., 2014). In a nutshell, in a location-cueing Posner Task, predictions are induced by the spatial cue, whose predictability affects uncertainty. Trial-wise cue predictability is usually inferred from recent trials (i.e., past experience) and impacts on RTs, requiring an update of the correspondent predictive model in case of novel information (Gómez et al., 2009).

Another behavioral paradigm to study adaptive attentive behavior is the Saccadic planning task (Go et al., 2022; O’Reilly et al., 2013), which we will refer to as “Location distribution task” in the following sections. Here, saccades are executed towards visual stimuli presented around a circular and typically imperceptible perimeter. Predictions are induced by varying spatial distributions of the saccade target stimuli (i.e., the mean and variance of a Gaussian distribution of the polar angle of the target coordinates). According to the task design, speeded saccades are elicited by the majority of targets as their locations are easily predicted after a sufficient number of trials by evaluating the current spatial distribution. A slowing of saccadic latencies is observed immediately after changes of the distribution when stimuli occur in unexpected circular locations. In an eye-tracking study, O’Reilly

and colleagues (2013) employed different types of unexpected events in order to segregate the updating process from the surprise response. In particular, responses to unexpected but informative saccadic targets (i.e., differently colored targets indicating a shift of the spatial distribution) were contrasted with unexpected but uninformative targets (i.e., grey-colored targets occasionally occurring outside of the current spatial distribution without signaling any change in the distribution, so-called “one-off” trials). Their findings suggested slower saccadic RTs for both types of surprising stimuli, whereas dwell time, which was the amount of time participants spent looking at the target, was only enhanced for unexpected informative stimuli signaling the need to update. In addition, Go and colleagues (2022) conducted two experiments demonstrating that eye movement metrics constitute a reliable index of internal model updating even when explicit change signals (such as different stimulus colors) are lacking.

It is generally accepted that eye movements are critically connected to covert attention shifts (Rizzolatti et al., 1987). Indeed, eye movements to a given location are necessarily preceded by covert attention shifts to this location, enhancing perceptual processing. Therefore, one could argue that the location-cueing Posner task and the Saccadic location distribution task involve shared cognitive processes. Along these lines, the %CV-dependent modulation of the validity effect in the Posner task can be observed with manual as well as saccadic responses to the targets (e.g., Dombert et al., 2016; Vossel, Mathys, et al., 2014). Both tasks should, therefore, allow the exploration of cognitive processes related to the generation and updating of predictive internal models within the visuospatial attentional system (O’Reilly et al., 2013). Hence, in the present study, two behavioral tasks were employed: a Posner cueing task and a Location distribution task. Both tasks were designed as saccadic eye-movement tasks and involved volatile probabilistic contexts to enable investigations of the updating of internal representations concerning cue-target relationships and spatial distribution of saccade targets, respectively. More precisely, experimental contingencies were embodied by unsignalled %CV changes during the Posner cueing task and by unsignalled mean and variance manipulations of target location distributions for the Location distribution task. These experimental contingencies were manipulated in order to

change unpredictably over time, with similar rates for both tasks, producing, for the Posner cueing task, a trial-by-trial uncertainty about the predictive value of the spatial cue and, for the Location distribution task, uncertainty about the saccadic target locations.

Therefore, the initial goal of the current study was to validate these modified versions of the two paradigms to reveal behavioral signatures of updating mechanisms of the respective internal models. We thus hypothesized that changes in cue predictability and in mean and variance distributions would be related to slower RTs in both tasks, respectively.

Moreover, although the behavioral tasks seem to tap into analogous cognitive processes, they have been linked to distinct functional correlates: functional magnetic resonance imaging (fMRI), transcranial magnetic stimulation (TMS), and event-related optical signal (EROS) evidence suggest that updating processes in the Posner task are strongly related to significant activity changes in the rTPJ (Geng & Vossel, 2013; Mengotti et al., 2017; Parisi et al., 2020; Vossel et al., 2015). On the contrary, fMRI evidence suggests that updating processes in the saccade planning task are strongly related to significant activity in the anterior cingulate cortex (ACC), whereas surprising but uninformative stimuli activate the intraparietal cortex (O'Reilly et al., 2013).

To address this functional inconsistency, we secondly aimed at investigating possible associations or dissociations among the signatures of predictive models updating at a behavioral level by having the same participants perform both types of tasks. In this perspective, correlational analyses were executed in order to test the degree of dependence of the two processes. Indeed, a direct behavioral investigation of potential correlations between the two predictive models is currently lacking.

2. MATERIALS AND METHODS

2.1 Participants

Thirty-five healthy volunteers participated in the study (21 males, 15 females; age range 24 – 40; mean age \pm standard deviation: 28.9 ± 3.9 years). They were all right-handed, as assessed by the Edinburgh Handedness Inventory (Oldfield, 1971),

had normal or corrected-to-normal vision, and had no past or present neurological or psychiatric disorders. All participants were naïve to the purpose of the experiment. The study was approved by the ethics committee of the German Psychological Society. It was conducted in accordance with the Code of Ethics of the World Medical Association (Declaration of Helsinki). Informed consent was obtained from all participants, who received a monetary reimbursement for participating in the experiment. Data from 9 and 11 participants had to be excluded from the Posner Cueing task and from the Location distribution task due to bad performance or bad eye tracking signal (i.e., the percentage of correct/analyzable trials was equal to or less than 70%). Therefore, the final sample for the Posner cueing task comprised 26 participants (mean age \pm standard deviation: 29.5 ± 4.3), while the final sample for the Location Distribution task comprised 24 participants (mean age \pm standard deviation: 29 ± 3.8). Finally, a sample of 22 participants with sufficient analyzable trials for both tasks was considered for correlation analyses (mean age \pm standard deviation: 29.3 ± 3.8).

2.2 Procedure and Apparatus

Each participant performed both behavioral tasks consecutively on the same day. The order of the tasks, which were interspersed by a 20-minute break, was alternated across participants. Both tasks were programmed and run using PsychoPy for Windows, version 2022.2.5. Stimuli were presented on a 15.6-inch monitor (spatial resolution 1680x1050, refresh rate 60 Hz) with a viewing distance of 60 cm. Participants sat in a dimly lit, sound-proof room with their heads stabilized by a chinrest, which was employed to reduce head movements.

Eye movements were recorded by means of an SR Research Eyelink 1000 desktop-mounted system, with a sampling rate of 1000 Hz. Before the beginning of each task, a 9-point eye-tracker calibration and validation were performed, with a maximum validation error of 1° visual angle. Only the right eye's position was monitored and analyzed. Once calibrated, participants were instructed to maintain their heads as still as possible on the chinrest to restrict head movements. A second calibration occurred shortly after half of each task. Prior to each task, a training

session was administered to familiarize participants with the tasks and let them practice proper and fast saccadic movements.

2.3 Stimuli and Experimental Paradigm

2.3.1 Posner cueing task

A location-cueing paradigm with central cueing (Posner, 1980) was employed. On each trial, two peripherally located boxes (50 pixels wide x 100 pixels high; 8° of eccentricity in each visual field), that could include target stimuli, were displayed. A central diamond was placed between them, acting as a fixation point. Subsequently, a triangle occurring for 200 ms was superimposed on the diamond, creating an arrowhead pointing to one of the peripheral boxes and serving as a spatial cue. After a 600 ms stimulus onset asynchrony, a black dot (13-pixel diameter) corresponding to the target appeared for 350 ms in one of the boxes. Three intertrial interval values were considered (2000, 2200, 2400 ms) and randomly occurred across trials (See Fig. 1A). Participants were instructed to maintain central fixation during the cue period and to avail of the cue to concentrate on the indicated location. They were asked to make a saccade toward the target as quickly as possible and they were asked to fixate back on the central diamond. Furthermore, they were encouraged to blink after their second saccade. The current task was characterized by block-wise changes between two levels of the percentage of cue validity (%CV). One level was 80%: within a block, 80% of trials were valid, that is, when the cue correctly predicted the target location, and 20% of trials were invalid, that is, when the target appeared within the uncued box. The second level of %CV was 50%: valid and invalid trials occurred equally often within a block. Participants were informed about both the predictive value of the cue and the possible changes in %CV over the task but were kept from the specific levels or when they would change, given that blocks were concatenated and not temporally separated (See Fig. 2).

In addition, another set of trials, called “one-offs,” were added. In these trials, the targets were differently colored (i.e., red dots) compared to regular black dot targets. Four one-off trials, two valid and two invalid, were incorporated in each block, independently from %CV (See Fig. 1B). Furthermore, participants were instructed

to perform the same task (i.e., performing a saccade toward the target as fast as possible) in case of one-off trials, being aware that they did not carry any meaning with regard to the task (i.e., no information about the predictive value of the cue). One-off trials were included to dissociate the effects of surprise from the process of updating an internal model. On one-off trials, we expected participants to be surprised by the unexpected target color without performing any kind of updating mechanism. Indeed, updating should only occur on the regular trials, since participants were explicitly informed that one-off trials had no predictive value relating to future trials. Twelve blocks were concatenated and presented as a continuous sequence, separated only by three breaks of 1 minute. Half of the block comprised 36 trials, while the other half comprised 26 trials, resulting in a total of 372 trials for the Posner Cueing task (See Fig. 2). Regular trials and one-off trials were pseudo-randomly intermixed within each single block. Each participant was presented with the same sequence of trials and the same sequence of blocks. The order of the blocks depended on both the %CV and the number of trials of each block. According to the former, blocks were alternated, starting with 80% CV, while they were pseudo-randomly distributed over the task according to the number of trials included (See Fig. 2). Considering each behavioral condition (i.e., valid 80%CV, invalid 80%CV, valid 50%CV, invalid 50%CV, valid one-off 80%CV, invalid one-off 80%CV, valid one-off 50%CV, invalid one-off 50%CV), right and left targets were equally distributed in each condition.

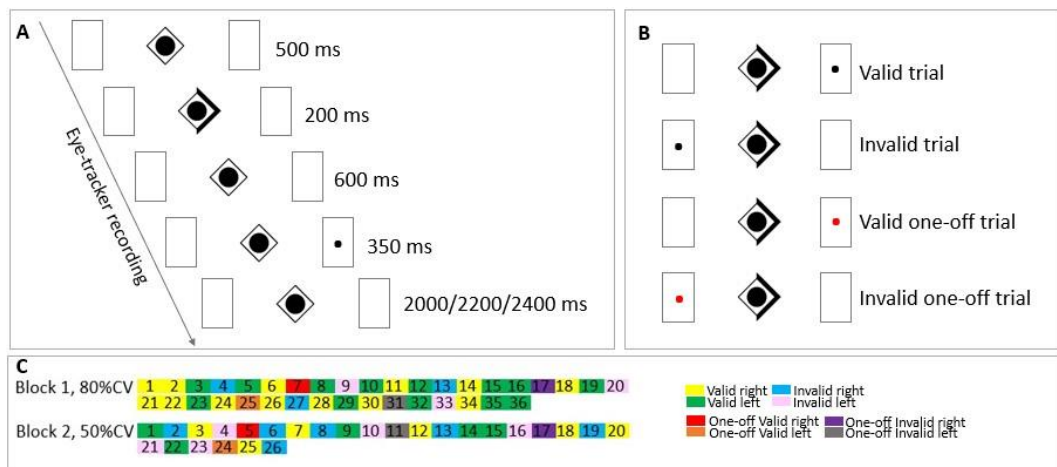


Figure 1. Posner cueing task experimental paradigm.

(A) Posner cueing task timeline for a validly cued trial. A central fixation diamond was positioned between two peripheral boxes, located at an eccentricity of 8° from the center to the inner edge along

the horizontal meridian. After 500 ms, a spatial cue, consisting of a triangle superimposed on the diamond and creating an arrowhead indicating towards one of the two boxes, occurred for 200 ms. A 600 ms stimulus onset asynchrony was then followed by the appearance of the target, corresponding to a black dot occurring within one of the boxes for 350 ms. Participants had to move their eyes toward the target as fast as possible within an intertrial interval of 2000, 2200, or 2400 ms. (B) Behavioral conditions of the Posner cueing paradigm. A valid trial, an invalid trial, a valid one-off trial, and an invalid one-off trial are shown. Regular trials were characterized by black targets while one-off trials were characterized by red targets. (C) Example of the experimental design. Block 1 and block 2 sequences of trials are reported.

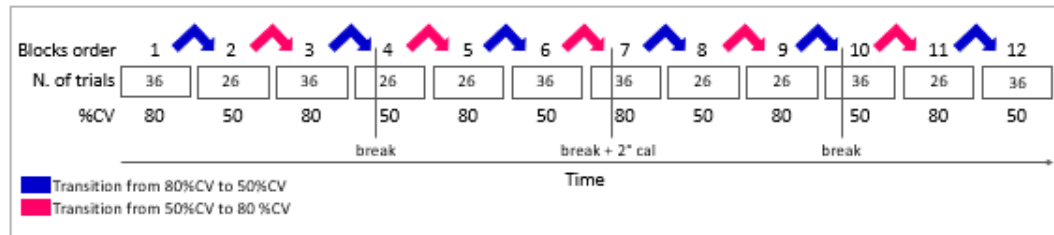


Figure 2. Cue validity changes in the Posner cueing task.

The task comprised 12 blocks. Each block included either 36 or 26 trials (regular and one-off trials), following the order reported in the figure. Alternating levels of %CV were employed, producing transitions from 80%CV to 50%CV and vice versa, as displayed in the figure. The timeline of the three breaks is shown. At the end of the second break, a second eye-tracker calibration was performed.

2.3.2 Location distribution task

A saccadic planning task without explicit spatial cues was employed, similar as in O'Reilly et al (2013) and Go et al. (2022). On each trial, two concentric circles were centrally displayed (the largest with a 650-pixel diameter while the smallest with a 550-pixel diameter), creating a circular region (100-pixel wide) between the two circle boundaries that included target stimuli. A central diamond acted as a fixation point. Subsequently, a non-spatial warning signal was presented by a 200 ms period of increasing brightness of the diamond perimeter. After a 600 ms stimulus onset asynchrony, a black dot (13-pixel diameter) corresponding to the target appeared for 350 ms in the middle of the circular region (i.e., 8° from central fixation). Three intertrial interval values were considered (2000, 2200, 2400 ms) and randomly occurred across trials (See Fig. 3A). Participants were instructed to maintain central fixation during the fixation period and to make a saccade toward the target as quickly as possible. Moreover, they were asked to fixate back on the central diamond and were encouraged to blink after this second saccade. Within each block, the target locations were established according to a circular Gaussian distribution with specific mean and variance values. In particular, eight mean and two variance

values were taken into account. Regarding the latter values, one was deemed to be large (i.e., 24°), and the other was deemed to be small (i.e., 8°). The current task was thus characterized by blockwise changes among saccade target location distributions. Indeed, twelve different spatial distributions comprising 32 or 22 spatial locations were drawn by manipulating mean and variance values. Importantly, all targets were equidistant from the central fixation, appearing along the circular region. Hence, each block was characterized by targets occurring in similar locations following pre-defined spatial distributions, thereby facilitating anticipation by the participants. Participants were informed that target locations could be similar but could also change over the task. However, they were kept from the precise distributions and when they would have changed, given that blocks were not temporally separated (See Fig. 4 and Fig. 5).

In addition, another set of trials, called “one-offs,” has been added. In these trials, targets were differently colored (i.e., red dots) compared to black dots targets. Four one-off trials were incorporated in each block: two one-off trials showed targets appearing within the experimental distribution of that block, while the other two showed targets appearing outside the experimental distribution of that block (See Fig. 3B). More precisely, the spatial coordinates of the two outside one-off targets were selected from two other different distributions with mean values of at least 3-means distance from the mean of the experimental distribution. Participants were instructed to perform the same task (i.e., performing a saccade toward the target as fast as possible) in case of one-off trials, being aware that they did not carry any meaning with regard to the task (i.e., no information about the experimental distribution). One-off trials were included to dissociate the effects of surprise from the process of updating an internal model. On one-off trials, we expected participants to be surprised by the unexpected target color without performing any kind of updating mechanism. Indeed, updating should only occur on the regular trials, since participants were explicitly informed that one-off trials had no predictive value relating to future trials.

Twelve blocks were concatenated and presented as a continuous sequence, separated only by three breaks of 1 minute. Half of the block comprised 36 trials, while the other half comprised 26 trials, resulting in a total of 372 trials for the

Location distribution task (See Fig. 4). Experimental trials and one-off trials were pseudo-randomly intermixed within each single block. Each participant was presented with the same sequence of trials and the same sequence of blocks. Blocks were pseudo-randomly distributed over the task according to the number of trials included.

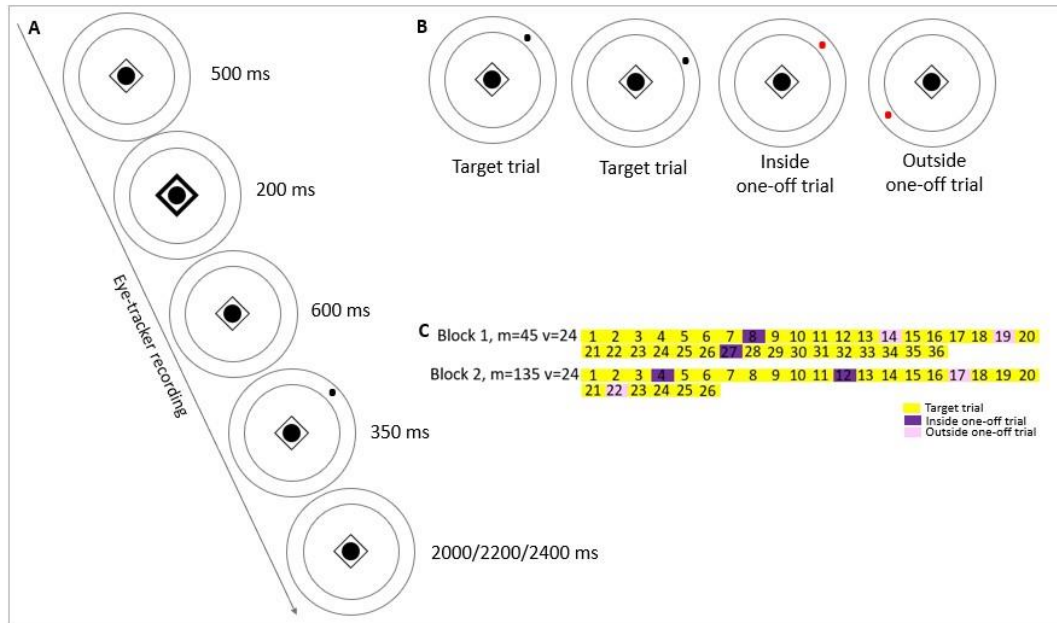


Figure 3. Location distribution task experimental paradigm.

(A) Location distribution task timeline. A central fixation diamond was positioned within two centered concentric circles. After 500 ms, a non-spatial warning signal, consisting of increasing brightness of the diamond perimeter, occurred for 200 ms. A 600 ms stimulus onset asynchrony was then followed by the appearance of the target, corresponding to a black dot occurring in the middle of the circular region created by the concentric circles for 350 ms. Participants had to move their eyes toward the target as fast as possible within an intertrial interval of 2000, 2200, or 2400 ms. (B) Behavioral conditions of the Location distribution task. Two target trials included in the same spatial distribution, an inside one-off trial and an outside one-off trial, are shown. Regular trials were characterized by black targets while one-off trials were characterized by red targets. (C) Example of the experimental design. Block 1 and block 2 sequences of trials are reported.

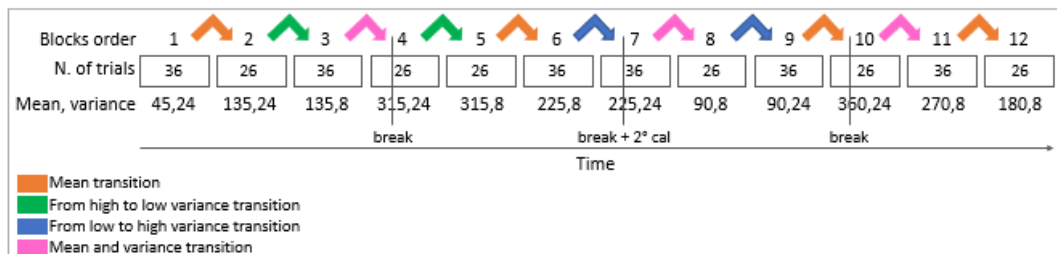


Figure 4. Location distribution changes in the Location distribution task.

The task comprised 12 blocks. Each block included either 36 or 26 trials (regular and one-off trials), following the order reported in the figure. Different values of mean and variance of the spatial distributions have been employed (they are listed in the figure), producing: mean transitions, from high to low variance transitions, from low to high variance transitions, and mean/variance

transitions, as displayed in the figure. The timeline of the three breaks is shown. At the end of the second break, a second eye-tracker calibration was performed.

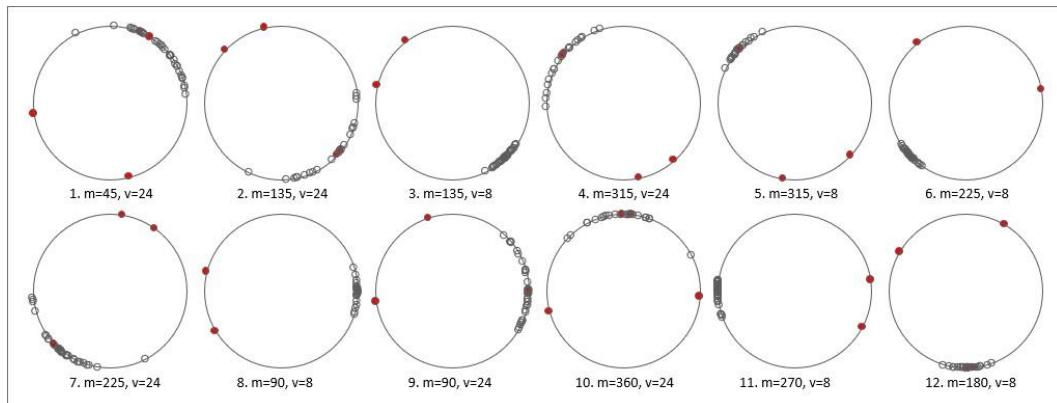


Figure 5. Target locations in the Location distribution task.

The target locations of each distribution are shown. Empty dots represent target trials, while red dots represent one-off trials (both inside and outside the distribution). The corresponding mean and variance values are mentioned for each distribution.

2.4 Eye Movement Data Analysis

For both tasks, eye movement data were preprocessed and analyzed using MATLAB 2023a, while behavioral statistical analyses were performed with Jamovi for Windows, version 1.6.23. Blinks, fixations, and saccades were identified by employing the Eyelink event parser with standard settings. Episodes during blinks were discarded. After the target occurrence, the first saccade towards the target was analyzed. Trials including first saccades with a latency of <90 ms (i.e., anticipated responses) and saccades subtending less than 100 pixels, were discarded. Moreover, in order to evaluate the accuracy of each saccade, the distance between the gaze coordinates at the central fixation and the actual central fixation coordinates at the start of the first saccade was calculated for each trial and needed to be within a 55-pixel region (i.e., 1.5°). Likewise, the distance between the gaze coordinates at the target at the end of the first saccade and the actual dot coordinates was calculated for each trial and needed to be within a 72-pixel region (i.e., 2°).

Saccadic RTs were considered for both tasks and defined as the latency between the target and the saccade onset. Generally, behavioral analyses were performed in order to investigate potential differences in the updating process during transitions among blocks.

2.4.1 Posner cueing task

In the current task, mean RTs were calculated separately for valid trials, invalid trials, valid one-off trials, and invalid one-off trials. For regular valid and invalid trials, mean RTs were calculated separately for the second and the first half of each 80%CV and 50%CV block (i.e., for the trials before and after a %CV change). Here, the first half of the first block and the second half of the last block were omitted since these trials were not preceded or followed by a %CV change. This resulted in eight different conditions: valid80-second half and invalid80-second half (before a transition to 50), valid50-second half and invalid50-second half (before a transition to 80), valid80-first half and invalid80-first half (after a transition from 50), valid50-first half and invalid50-first half (after a transition from 80). Accordingly, mean RTs were entered in a three-way repeated-measures analysis of variance (ANOVA) by considering validity condition (valid, invalid), %CV (80, 50), and half (first half, second half) as within-subject factors. Where needed, post-hoc t-tests were applied.

Moreover, mean RTs of valid one-off trials were contrasted with mean RTs of valid regular trials, independently from behavioral conditions, by using a paired-sample t-test. A second t-test was conducted to compare invalid one-off trials and invalid regular trials, independently from behavioral conditions. This was done to test if the surprise by rare color changes was reflected in RTs in one-off trials.

2.4.2 Location distribution task

With respect to this task, mean RTs were calculated separately for regular target trials, inside one-off trials, and outside one-off trials for each block. For regular trials, mean RTs were calculated for the second and first half of each distribution block (i.e., for the trials before or after a change in the mean and/or variance of the distribution), separately for trials before/after a change in the mean of the distribution, a change from a high (24°) to a low (8°) variance, a change from a low (8°) to a high (24°) variance or a change in both mean and variance. The first half of the first block and the second half of the last block were omitted since these trials were not preceded or followed by a distribution change. This resulted in 8 conditions: mean-second half (before a mean change), mean-first half (after a mean

change), variance high-low-second half (before a high-low variance change), variance high-low-first half (after a high-low variance change), variance low-high-second half (before a low-high variance change), variance low-high-first half (after a low-high variance change), mean/variance-second half (before a mean/variance change), mean/variance-first half (after a mean and a variance change). Accordingly, mean RTs were entered in a two-way ANOVA considering the transition type (mean, variance²⁴, variance⁸, mean/variance) and half (first half, second half) as within-subject factors. Where needed, post-hoc t-tests were applied. Moreover, mean RTs of regular trials, inside and outside one-off trials, were entered in a repeated-measures ANOVA without dividing them into halves and considering RTs as the within-subject factor to test for an effect of the rare color changes of the target.

2.4.5 Correlations

In order to determine the degree of a possible association between the updating processes evoked by the two behavioral tasks, two variables relating to the Posner cueing task and three variables relating to the Location distribution task were considered. More precisely, we calculated the difference between the VE in the second half of 80%CV blocks and the VE in the first half of the 50%CV blocks. Similarly, we extracted the second variable by computing the difference between the VE in the second half of 50%CV blocks and the VE in the first half of the 80%CV blocks. Regarding the Location distribution task, the difference between the RTs related to the mean-second half (before a mean change) and the mean-first half (after a mean change) was calculated. In addition, we computed the difference between the RTs related to the variance high-low-second half (before a high-low variance change) and the variance high-low-first half (after a high-low variance change), along with the difference between the RTs related to the variance low-high-second half (before a low-high variance change) and the variance low-high-first half (after a low-high variance change). Eventually, these variables reflecting transition effects (i.e., the differences in VEs for the Posner cueing task and the differences in RTs for the Location distribution task) were entered into a Spearman's correlation analysis in order to have a measure of whether and how

much behavioral outcomes of the two tasks, specifically reflecting updating mechanisms, were related.

3. RESULTS

3.1 Posner cueing task

The repeated measures ANOVA conducted on mean RTs before or after a %CV change did not reveal a significant main effect either of the %CV ($F(1,25) = 2.180$, $p = 0.152$, $\eta^2 = 0.080$) or the half factor ($F(1,25) = 1.270$, $p = 0.271$, $\eta^2 = 0.048$). Likewise, neither the interaction between the validity condition and the %CV factor ($F(1,25) = 1.007$, $p = 0.325$, $\eta^2 = 0.039$) nor the interaction between the validity and half ($F(1,25) = 0.665$, $p = 0.423$, $\eta^2 = 0.026$), nor the interaction between %CV and the half factor ($F(1,25) = 0.120$, $p = 0.732$, $\eta^2 = 0.005$) reached statistical significance. In contrast, this analysis showed a significant main effect of validity ($F(1,25) = 18.044$, $p < 0.001$, $\eta^2 = 0.419$) and a significant three-way interaction between validity, %CV, and half ($F(1,25) = 8.019$, $p = 0.009$, $\eta^2 = 0.243$). This interaction reflects a differential modulation of RTs in valid and invalid trials by %CV in the first and second half of each %CV block, a pattern that would be expected if participants indeed inferred the unsignalled changes in %CV from recent observations.

In order to elucidate the origin of this interaction, post-hoc t-tests were performed, suggesting a statistically significant RT difference between valid and invalid trials in the second half of 80%CV blocks ($t(25) = -4.927$, $p < 0.001$). Conversely, this difference was not significant in the first half, i.e. immediately after a 50%CV block ($t(25) = -1.998$, $p = 0.057$). The difference in RTs between valid and invalid trials (i.e., the VE) was significantly higher in the second half of blocks with a %CV of 80 (19.89 ms), compared to the first half of blocks with the same cue-validity (9.89 ms). This can be attributed to the fact that in the 80%CV second halves, participants had already learned the higher probability of target occurrence in the cued location. This was not the case in the first halves of blocks following blocks where the cue was unpredictable, and during which they were still learning and updating the higher %CV level.

Then, mean RTs of the valid50-second half and mean RTs of the invalid50-second half were revealed to be significantly different ($t(25) = -2.69$, $p = 0.013$). This result reflects the fact that even with a low but learned (since we are considering the second half of the blocks) %CV valid trials are faster than invalid trials. However, this difference (9 ms) was statistically smaller than the difference we found between valid and invalid trials in blocks with a higher %CV (i.e., 80-second half with 19.89 ms VE). For the first half, there was no statistical difference between the VE in the 50% and the 80% condition.

With respect to the difference in RTs between the valid50-first half and the invalid50-first half, it was shown to reach statistical significance ($t(25) = 3.773$, $p < 0.001$) with valid trials faster than invalid trials (14.1ms VE). This finding could be explained by the lingering influence of the preceding high %CV block.

Another important finding related to the implementation of the updating process would have been the comparison between mean RTs of the invalid80-second half and the invalid80-first half, given that updating should be more elicited by invalid trials. However, our data did not show a statistical difference ($t(25) = 1.527$, $p = 0.139$), although it is possible to notice a qualitative discrepancy between the two parameters (213 ms versus 206 ms).

Figure 5 summarizes the effects of %CV transitions on RTs in the Posner cueing task. Overall, our findings revealed behavioral responses in accordance with the existing literature, according to which valid trials yield faster RTs than invalid trials. This was especially true when the %CV was higher (i.e., 80), but only in the second half of the hidden %CV blocks (i.e., when %CV had been learned). Thereby, our results disclosed the implementation of updating participants' internal models about cue-target contingencies, emerging straight after transitions from a %CV to the other. (See Table 1 for statistics)

Finally, we carried out two t-tests on the mean RTs of valid one-off trials and invalid one-off trials, comparing them to mean RTs of valid regular trials and invalid regular trials, respectively. Neither of the two analyses reached statistical significance ($t(25) = -0.77$, $p = 0.449$; $t(25) = -0.61$, $p = 0.545$), indicating that the infrequent color changes did not affect RTs.

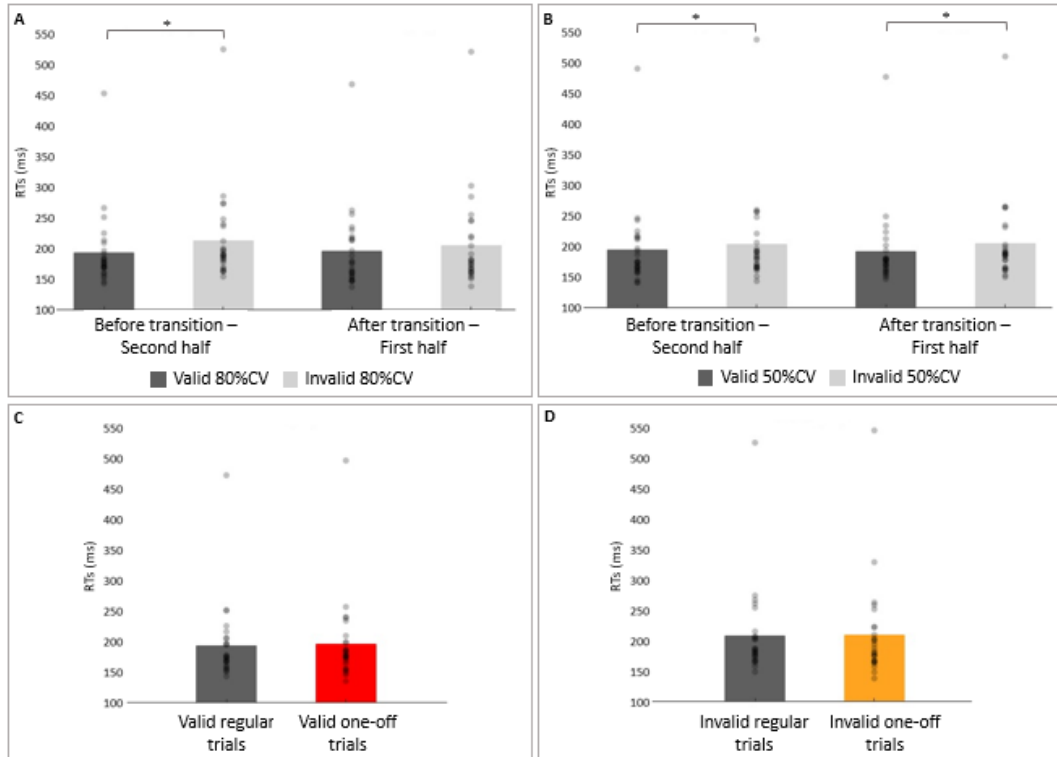


Figure 5. Posner cueing task results

(A) Mean response times of the 80%CV are plotted as a function of both validity and half conditions. Significant effects are marked with asterisks. (B) Mean response times of the 50%CV are plotted as a function of both validity and half conditions. Significant effects are marked with asterisks. (C) Mean response times are plotted considering the comparison between valid regular trials and valid one-off trials. (D) Mean response times are plotted considering the comparison between invalid regular trials and invalid one-off trials. For each condition of each graph, individual data are plotted (grey dots) along with averaged values.

Table 1. Results of post-hoc t-tests of the Posner cueing task Anova

<i>Validity</i>	<i>%CV</i>	<i>Half</i>	<i>Validity</i>	<i>%CV</i>	<i>Half</i>	<i>dof</i>	<i>t</i>	<i>p</i>
valid	80	before	valid	80	after	25	-0.616	0.544
"	"	"	invalid	80	before	25	-4.927	<.001
"	"	"	invalid	80	after	25	-2.536	0.018
"	"	after	invalid	80	before	25	-2.96	0.007
"	"	"	invalid	80	after	25	-1.998	0.057
"	50	before	valid	50	after	25	1.394	0.176
"	"	"	invalid	50	before	25	-2.69	0.013
"	"	"	invalid	50	after	25	-2.253	0.033
"	"	after	invalid	50	before	25	-3.958	<.001
"	"	"	invalid	50	after	25	-3.773	<.001
invalid	80	before	invalid	80	after	25	1.527	0.139
"	"	"	invalid	50	before	25	2.682	0.013
"	50	before	invalid	50	after	25	0.629	0.629

Red-coloured p-values represent statistically significant results, while black-coloured p-values represent statistically insignificant results. Bold p-values (in both red and black) represent results that have been reported in the text.

3.2 Location distribution task

The repeated measures ANOVA conducted on mean RTs before and after mean and/or variance changes of the distribution indicated a significant main effect of both the transition type ($F(1,25) = 4.92$, $p = 0.004$, $\eta^2 = 0.176$) and the half factor ($F(1,25) = 10.40$, $p = 0.004$, $\eta^2 = 0.311$). Moreover, a significant interaction between the transition type and the half factor was observed ($F(1,25) = 5.34$, $p = 0.002$, $\eta^2 = 0.188$).

Subsequent post-hoc t-tests suggested a statistically significant difference between RTs before and after a change of the distribution mean ($t(23) = -5.120$, $p < 0.001$), pointing out considerably slower RTs after a change, i.e. the need to update the internal model about the new spatial distribution. On the contrary, comparing the second and first half of blocks during a variance change did not reach statistical significance (i.e., high-low variance change: $t(23) = 0.984$, $p = 0.336$; low-high variance change: $t(23) = 0.088$, $p = 0.931$). Hence, variance shifts did not produce significant RT changes in the present task. In addition, there were significant RT differences between low and high variance distributions in the second half of the respective blocks ($t(23) = 2.265$, $p = 0.033$), unveiling that participants were faster in making saccades toward targets within a spatial distribution with small variance (177.16 ms) as opposed to targets within a spatial distribution with a large variance (190.18 ms), preserving the mean value.

No significant difference between RTs before or after a mean and variance change was observed ($t(23) = -1.384$, $p = 0.180$). (See Tab. 2 for statistics).

Taken together, these findings highlighted a slowing in RTs when the mean value of the distributions changed, reflecting the updating process about the new spatial locations of the saccade targets. Moreover, different behaviors have been pointed out according to the variance value of the distribution: after learning of the variance distributions, participants executed faster saccadic movements in case of a smaller variance compared to a larger one.

Finally, the ANOVA executed on the mean RTs related to regular trials, and one-off trials appearing inside and outside the current spatial distribution, indicated a statistically significant difference ($F(1,23) = 47.2$, $p < 0.001$, $\eta^2 = 0.080$). Further post hoc tests showed that one-off outside trials were significantly slower than both

regular and one-off inside trials ($t(23) = -7.205$, $p < 0.001$; $t(23) = -7.174$, $p < 0.001$), while the latter two did not reveal any statistical difference ($t(23) = 0.721$, $p = 0.478$). This final analysis pointed out that the position, including one-off trials, affected behavioral performances by increasing RT costs when targets appeared outside the underlying spatial distribution. In contrast, color changes did not have any impact on them. Figure 6 summarizes the results of the transition effects on RTs in the Location distribution task.

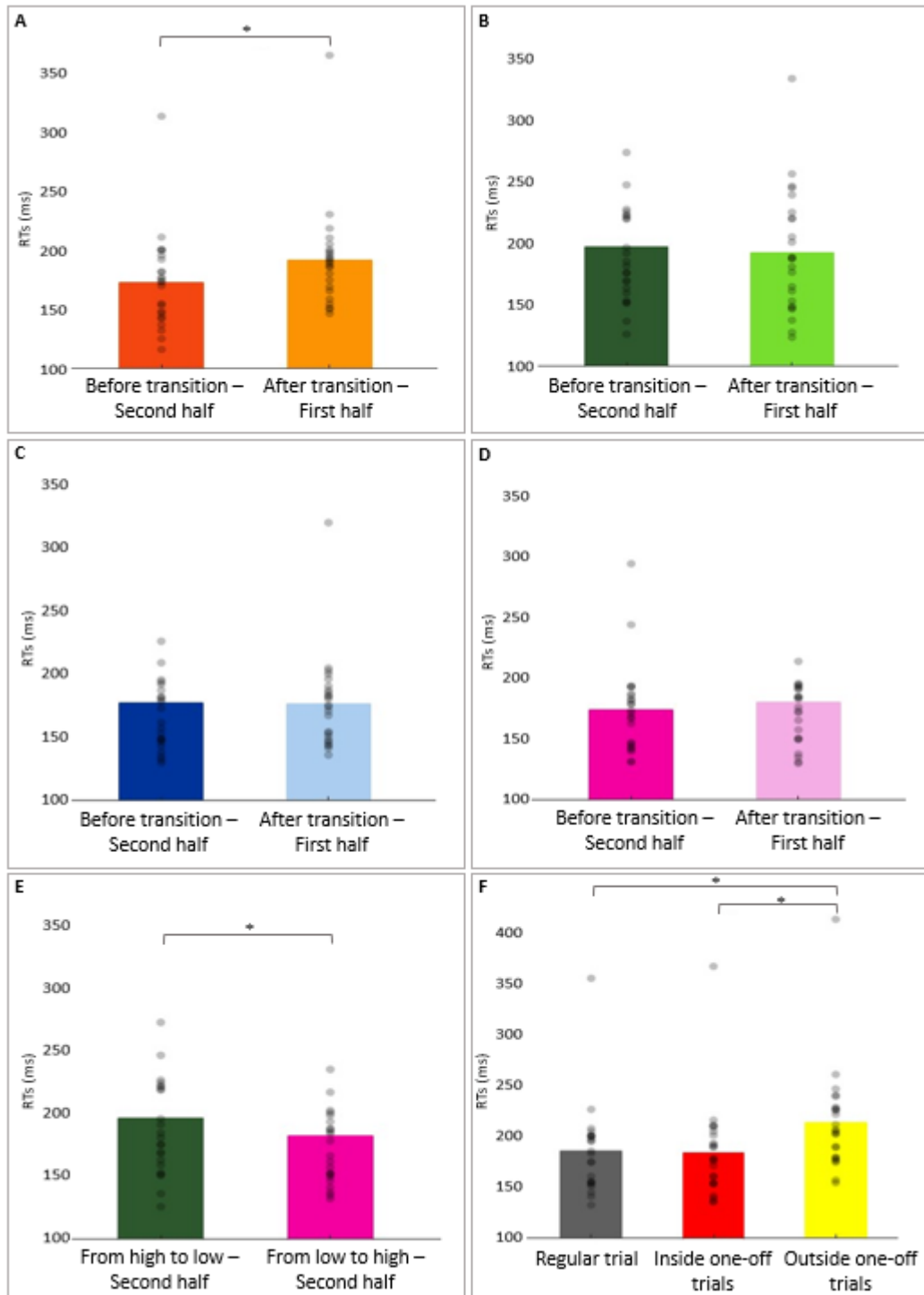


Figure 6. Location distribution task results.

Mean response times are plotted as a function of half condition and transition conditions. Significant effects are marked with asterisks (A) Mean transition. (B) From high variance to low variance transition. (C) From low variance to high variance transition. (D) Mean/variance transition. (E) Mean response times are plotted considering the comparison between low and high variance distributions in the second half of the respective blocks. Significant effects are marked with asterisks. (F) Mean response times are plotted considering the comparison between regular, inside one-off, and outside one-off trials. Significant effects are marked with asterisks. For each condition of each graph, individual data are plotted (grey dots) along with averaged values.

Table 2. Results of the Location distribution task Anova

<i>Transition</i>	<i>Half</i>	<i>Transition</i>	<i>Half</i>	<i>dof</i>	<i>t</i>	<i>p</i>
mean	before	mean	after	23	-5.120	<.001
var1	before	var1	after	23	0.984	0.336
"	"	var2	before	23	2.265	0.033
"	after	var2	before	23	1.216	0.236
"	"	var2	after	23	1.82	0.082
var2	before	var2	after	23	0.088	0.931
mv	before	mv	after	23	-1.384	0.180

Red-coloured p-values represent statistically significant results, while black-coloured p-values represent statistically insignificant results. Bold p-values (in both red and black) represent results that have been reported in the text.

3.3 Correlations

The correlation analysis taking into consideration the VE differences from transitions from 80 to 50% and vice versa (considering the second half and the first half, respectively) and the RT differences between second halves and first halves of the same transition type (i.e., mean, high-low variance, low-high variance) did not show any significant correlation effects (see Table 3 for statistics). These findings may suggest that the updating process, raised by specific Posner cueing task manipulations, is disjoint from the updating process raised by manipulations of the Location distribution paradigm.

Table 3. Results of the correlation analysis

	diffVE_80_50	diffVE_50_80
diff_means	r = 0.038 p = 0.868	r = 0.013 p = 0.956
diff_highVar	r = -0.199 p = 0.372	r = 0.076 p = 0.736
diff_lowVar	r = -0.199 p = 0.372	r = 0.152 p = 0.498

4. DISCUSSION

Mental models are built according to the frequency and prevalence of previous experience with the purpose of understanding and interfacing with environmental contexts. However, when new events occur within the same context but without being reflected by the current model, this latter needs to be updated in order to allow correct future predictions and behavior (Filipowicz et al., 2018). In this perspective, the present study sought to cast light on the behavioral signatures of the ability to build and mostly update one's internal model in the context of attentional selection.

To do so, we availed of two behavioral paradigms, which have been used to investigate these cognitive mechanisms, namely the Posner cueing task and the Location distribution task. Briefly, the former is characterized by a spatial predictive cue whose trial-by-trial predictability can be inferred from trial history, affecting RTs of the following trials. In other words, mental models about cue reliability are created and constantly updated during the execution of a Posner task with volatile cue-target contingencies. With respect to the Location distribution task, it is characterized by saccadic targets whose locations can be inferred by estimating the underlying spatial distribution. Again, behavioral outcomes, such as RTs of trials subsequent to changes in the distribution, appear to be influenced by updating internal models about the future target spatial distribution.

Therefore, utilizing modified variants of both tasks with saccadic responses, we intended to characterize and compare their behavioral signatures of model updating in the visuospatial attentional system. Of importance, close attention was paid to design both tasks and manipulate conditions to make them as similar as possible while preserving their typical traits. Firstly, analogous graphical elements were selected for both tasks: the central fixation diamond and the targets exhibited the same physical features, and targets were positioned at the same distance from the centre. In addition, the temporal distribution of events within a single trial was identical for both tasks, along with the equal total number of blocks and trials and the number of trials for each block (except for the last four blocks). Also, concerning the inclusion of one-off trials, we tried to achieve the highest similarity between the two tasks: each block had a constant number of one-off trials, and valid and invalid one-off trials were considered equivalent to inside and outside one-off trials, respectively. Moreover, there was an important consistency in their physical and abstract characteristics: they invariably consisted of red dots, and although participants were requested to execute fast saccades toward them, they did not carry any relevant information with regard to changes in cue validity or location distribution in both tasks. Finally, task instructions were nearly the same: participants had to move their eyes as quickly as possible to the targets, trying to predict their future locations according to previous experience and keeping in mind that changes could occur unpredictably over the course of both tasks.

Besides task features specifically related to the experimental paradigm and design, the same preprocessing and data analyses were performed in both tasks. Our behavioral analyses focused on mean saccadic RTs before and after a change in %CV and in mean and/or variance of the spatial distribution for, respectively, the Posner cueing task and the Location distribution task. As to the former, the present findings provided evidence supporting the distinct modulation of RTs by validity, %CV, and block half. More in detail, considering the second half of both 80 and 50%CV, valid trials were associated with significantly faster RTs compared to invalid trials. These data highlighted the typical benefit of orienting attention to cued locations and the cost of reorienting resources to unexpected target locations. Importantly, this result describes RTs of second halves as reflecting already learned and updated internal models about cue-target relationships, even when the %CV level was low (i.e., 50). However, the difference in RTs between valid and invalid trials was significantly higher in the highest %CV level (i.e., 80). This evidence is totally in agreement with previous literature showing that higher VEs derive from higher %CV (Vossel, Mathys, et al., 2014). Concomitantly, the absence of significant RT differences between invalid and valid trials in the first half of 80%CV could represent the moment in which participants were truly learning and updating the current %CV from the preceding unpredictable (50%) block. Taken together, these findings corroborate the adequacy of our saccadic version of the Posner cueing task in unveiling behavioral signatures of updating mechanisms.

Regarding the Location distribution task, the current results sustained distinct modulations of RTs before or after changes in distributional characteristics. In particular, taking into consideration the mean transition (i.e., switches to new target locations), we discovered significantly slower RTs after a change. When targets are presented in different locations than the ones included in the previous distribution, these new target locations are considered unexpected and require longer behavioral responses, reflecting the need to reorient attentional resources and update the internal model accounting for the new spatial distribution (i.e., during the first half of our blocks after mean transition). Regarding variance changes, we did not find any significant differences in RTs, likely owing to the small difference between target coordinates generating a weak updating process and precluding it from being

behaviorally revealed. However, once the variance of the distribution was learned (i.e., during the second half of before both variance transitions), we found faster saccades toward the targets when the variance was smaller as opposed to when it was larger, reflecting that also the variance was learned to some extent in this study. Taken together, these findings corroborate the adequacy of our saccadic version of the Location distribution task in unveiling the behavioral signatures of updating mechanisms.

The present findings were expanded by RT analyses of one-off trials, which were characterized by an irrelevant color change of the target. Firstly, our one-off trials were designed partially differently from one-off trials in the study by O'Reilly et al., (2013). In their task, the authors included one-off trials only outside the current distribution, considering them as surprising stimuli and comparing them to regular and updating trials. In the present Location distribution task, one-off trials were included both inside and outside the spatial distributions, to make them comparable with one-off trials in the Posner task, appearing at validly and invalidly cued locations. Our results from both tasks indicated that task-irrelevant color changes per se did not influence RTs. Location distribution task results further confirmed this evidence, by highlighting an impact on RTs only when one-off trials occurred outside the current spatial distribution, which was thus due to the unexpected target location instead of color change. Go et al. (2022) used another manipulation to introduce rare surprising, but task-irrelevant events. In a small proportion of trials, they presented the saccade targets nearer or further away from the location of regular trials, but within the current spatial distribution of target locations. As in our study, these low probability events were also not associated with increased RTs. The correlational analysis on measures from regular trials did not show any significant associations between updating processes investigated by our two tasks. In other words, changes in the validity effect after cue validity changes in the Posner cueing task were not related to RT changes after mean or variance changes in the Location distribution task. We believe that this absence of dependence could be that despite their similarity, the model representations still differ for the two tasks. More precisely, the generation and updating of mental models in the Posner cueing task involve experience containing more abstract information, i.e., the relationship

between two stimuli (cue and target), and accordingly requiring further processes, such as the interpretation of the cue. In contrast, the generation and updating of mental models in the Location distribution task involve experience containing more low-level information, i.e., the physical location of the target. Thus, we can speculate that this built-in distinction prevented us from finding possible associations between the two paradigms.

Alternatively, statistical power could have been too low to detect significant associations, since only data from 22 participants could be included in the correlation analyses. Moreover, future analyses should also consider dwell times, since this saccadic metric has been found to be specifically related to the updating process rather than to mere surprise (Go et al., 2022; O'Reilly et al., 2013). These data could disclose further evidence about the comparability of the cognitive processes in the two tasks. Finally, analyses using formal computational modeling could contribute to evaluating correlations between updating parameters. Specifically, participant-specific updating parameters can be derived from formal learning models of cue validity and saccadic location. Hence, performing correlations between these parameters would constitute a really interesting next step.

5. CONCLUSIONS

In the present study, we administered two behavioral tasks that were designed as saccadic eye-movement tasks and involved volatile probabilistic contexts with the aim of investigating the updating of their internal representations. Overall, our data demonstrated that our Posner cueing task version enabled us to examine the behavioral markers of updating internal models about trialwise cue validity and that our Location distribution task version let us explore the behavioral markers of updating internal models about the underlying spatial distribution of target locations. By comparing specific parameters from the two tasks, we did not find any correlational interplay between performances. These analyses should be expanded with examinations of dwell times and computational modeling of the updating process.

GENERAL CONCLUSIONS

Overall, the current studies represent significant findings in line with the existing literature along with providing novel insights into the knowledge about visuospatial attentional processes. Despite the robust interest in exploring this field and the huge amount of evidence, some questions remain unanswered. Our innovative methodologies together with specific behavioral paradigms let us expand the currently available data.

By availing of one of the most cutting-edge methods, represented by the EROS technique, we conducted the first experiment whereby we could uncover the neural underpinnings of endogenous orienting and reorienting, coinciding with a dorso-visual dialogue, responsible for both attentional processes. Moreover, our data support the contribution of ITPJ in deploying attention after the occurrence of a central predictive cue. Interestingly, our results indicated the contribution of rTPJ in the post-perceptual mechanism of updating internal expectations about the cue-target relationship depending on forthcoming events.

Following the first experiment results, in the second study, we wanted to further investigate the exact role of rTPJ by interfering with its activity via an rTMS experimental procedure. By observing the effects exerted by the rTMS stimulation on behavioral outcomes, we could thus consolidate the critical involvement of rTPJ in updating the predictive value ascribed to the spatial cue, on a trial-by-trial basis. Finally, in order to better understand the neural implementation of one of the central mechanisms included in this thesis, such as the ability to update one's contextual models, a behavioral study was carried out. Indeed, in the third experiment, participants underwent two behavioral tasks designed as saccadic eye-movement tasks and specifically manipulated in order to disclose the behavioral markers of updating internal models about, from one side, the trialwise cue validity and, from the other side, spatial distributions of target locations.

To conclude, taken together our results offer a unifying perspective to explain the behavioral and spatiotemporal dynamics of visuospatial attentional mechanisms, comprising attentional endogenous orienting, reorienting and updating of internal models. More precisely, besides being in line with the current literature by

demonstrating the critical contribution of specific dorso-parietal regions, such as bilateral SPL and, to a lesser extent, IPS, the functional results of Experiment 1 are totally consistent with Experiment 2 findings regarding rTPJ engagement in visuospatial mechanisms. Both studies, indeed, sustain the contextual updating theory (Geng and Vossel 2013) which, in turn, supports the crucial implication of rTPJ in updating one's mental models about the attentional contingencies (i.e., the predictive relationships between endogenous cues and subsequent visual stimuli) instead of describing rTPJ as a circuit-breaker component triggering the reorientation of attention. If in Experiment 1, the involvement of rTPJ in predictive and mutual relationships with dorso-visual brain areas has been highlighted at late time windows, letting us discard the possibility of rTPJ to be involved in the pure reorienting process, Experiment 2 directly indicated rTPJ contribution to the updating function, congruently considering very similar timings of activation. Our interpretations are still more supported by the consistency of the behavioral tasks we employed in both studies: two very similar variants of the Posner paradigm. The latter is widely known to be deeply suitable for investigating these attentional processes, but its specific eligibility has been further demonstrated by the third experiment shown in this thesis. Behavioral data resulting from our saccadic version of the Posner paradigm indicated a behavioral and temporal implementation of the updating mechanism elicited by the task at hand. We thus believe that our final conclusions rely on reliable and solid experimental designs, methodologies and subsequent data analyses.

REFERENCES

- Abrahamse, E. L., & Silvetti, M. (2016). Commentary: The Role of the Parietal Cortex in the Representation of Task-Reward Associations. *Front Neuroscience Neuroscience*. <https://doi.org/10.1038/nrn755>
- Ahrens, M. M., Veniero, D., Freund, I. M., Harvey, M., & Thut, G. (2019). Both dorsal and ventral attention network nodes are implicated in exogenously driven visuospatial anticipation. *Cortex*, *117*, 168–181. <https://doi.org/10.1016/j.cortex.2019.02.031>
- Arjona, A., Escudero, M., & Gómez, C. M. (2014). Updating of attentional and premotor allocation resources as function of previous trial outcome. *Scientific Reports*, *4*. <https://doi.org/10.1038/srep04526>
- Arjona, A., & Gómez, C. M. (2011). Trial-by-trial changes in a priori informational value of external cues and subjective expectancies in human auditory attention. *PLoS ONE*, *6*(6). <https://doi.org/10.1371/journal.pone.0021033>
- Arjona, A., & Gómez, C. M. (2013). Sequential Effects in the Central Cue Posner Paradigm: On-line Bayesian Learning. *Cognitive Electrophysiology of Attention: Signals of the Mind*, 45–57. <https://doi.org/10.1016/B978-0-12-398451-7.00004-X>
- Arjona, A., Rodríguez, E., Morales, M., & Gómez, C. M. (2018). The influence of the global/local probability effect on the neural processing of cues and targets. A functional systems approach. *International Journal of Psychophysiology*, *134*(December 2017), 52–61. <https://doi.org/10.1016/j.ijpsycho.2018.10.005>
- Arjona Valladares, A., Gómez González, J., & Gómez, C. M. (2017). Event related potentials changes associated with the processing of auditory valid and invalid targets as a function of previous trial validity in a Posner's paradigm. *Neuroscience Research*, *115*, 37–43. <https://doi.org/10.1016/j.neures.2016.09.006>
- Arridge, S. R., & Schweiger, M. (1995). <title>Sensitivity to prior knowledge in optical tomographic reconstruction</title> In B. Chance

& R. R. Alfano (Eds.), *Optical Tomography, Photon Migration, and Spectroscopy of Tissue and Model Media: Theory, Human Studies, and Instrumentation* (Vol. 2389, pp. 378–388). SPIE.

<https://doi.org/10.1117/12.209988>

- Baniqued, P. L., Low, K. A., Fabiani, M., & Gratton, G. (2013). Frontoparietal traffic signals: A fast optical imaging study of preparatory dynamics in response mode switching. *Journal of Cognitive Neuroscience*, *25*(6), 887–902. https://doi.org/10.1162/jocn_a_00341
- Baniqued, P. L., Low, K. A., Fletcher, M. A., Gratton, G., & Fabiani, M. (2018). Shedding light on gray(ing) areas: Connectivity and task switching dynamics in aging. *Psychophysiology*, *55*(3), e12818. <https://doi.org/10.1111/psyp.12818>
- Blanke, O., Mohr, C., Michel, C. M., Pascual-Leone, A., Brugger, P., Seeck, M., Landis, T., & Thut, G. (2005). Linking out-of-body experience and self processing to mental own-body imagery at the temporoparietal junction. *Journal of Neuroscience*, *25*(3), 550–557. <https://doi.org/10.1523/JNEUROSCI.2612-04.2005>
- Bressler, S. L., Tang, W., Sylvester, C. M., Shulman, G. L., & Corbetta, M. (2008). Top-down control of human visual cortex by frontal and parietal cortex in anticipatory visual spatial attention. *Journal of Neuroscience*, *28*(40), 10056–10061. <https://doi.org/10.1523/JNEUROSCI.1776-08.2008>
- Capotosto, P., Babiloni, C., Romani, G. L., & Corbetta, M. (2012). Differential Contribution of Right and Left Parietal Cortex to the Control of Spatial Attention: A Simultaneous EEG-rTMS Study. *Cerebral Cortex*, *22*(2), 446–454. <https://doi.org/10.1093/cercor/bhr127>
- Caspers, S., Geyer, S., Schleicher, A., Mohlberg, H., Amunts, K., & Zilles, K. (2006). The human inferior parietal cortex: Cytoarchitectonic parcellation and interindividual variability. *NeuroImage*, *33*(2), 430–448. <https://doi.org/10.1016/j.neuroimage.2006.06.054>
- Catani, M., Robertsson, N., Beyh, A., Huynh, V., de Santiago Requejo, F., Howells, H., Barrett, R. L. C., Aiello, M., Cavaliere, C., Dyrby, T. B., Krug, K., Ptito, M., D'Arceuil, H., Forkel, S. J., & Dell'Acqua, F. (2017). Short

- parietal lobe connections of the human and monkey brain. *Cortex*, *97*, 339–357. <https://doi.org/10.1016/j.cortex.2017.10.022>
- Chiarelli, A. M., Di Vacri, A., Romani, G. L., & Merla, A. (2013). Fast optical signal in visual cortex: Improving detection by General Linear Convolution Model. *NeuroImage*, *66*, 194–202. <https://doi.org/10.1016/j.neuroimage.2012.10.047>
- Chiarelli, A. M., Maclin, E. L., Low, K. A., Fabiani, M., & Gratton, G. (2015). Comparison of procedures for co-registering scalp-recording locations to anatomical magnetic resonance images. *Journal of Biomedical Optics*, *20*(1), 016009. <https://doi.org/10.1117/1.jbo.20.1.016009>
- Chiarelli, A. M., Romani, G. L., & Merla, A. (2014). Fast optical signals in the sensorimotor cortex: General Linear Convolution Model applied to multiple source-detector distance-based data. *NeuroImage*, *85*, 245–254. <https://doi.org/10.1016/j.neuroimage.2013.07.021>
- Chica, A. B., Bartolomeo, P., & Lupiáñez, J. (2013). Two cognitive and neural systems for endogenous and exogenous spatial attention. *Behavioural Brain Research*, *237*(1), 107–123. <https://doi.org/10.1016/j.bbr.2012.09.027>
- Chica, A. B., Bartolomeo, P., & Valero-Cabré, A. (2011). Dorsal and ventral parietal contributions to spatial orienting in the human brain. *Journal of Neuroscience*, *31*(22), 8143–8149. <https://doi.org/10.1523/JNEUROSCI.5463-10.2010>
- Corbetta, M., Kincade, J. M., Ollinger, J. M., McAvoy, M. P., & Shulman, G. L. (2000). Voluntary orienting is dissociated from target detection in human posterior parietal cortex. *Nature Neuroscience*, *3*(3), 292–297. <https://doi.org/10.1038/73009>
- Corbetta, M., Patel, G., & Shulman, G. L. (2008). The Reorienting System of the Human Brain: From Environment to Theory of Mind. In *Neuron* (Vol. 58, Issue 3, pp. 306–324). Cell Press. <https://doi.org/10.1016/j.neuron.2008.04.017>
- Corbetta, M., & Shulman, G. L. (2002). Control of goal-directed and stimulus-driven attention in the brain. *Nature Reviews Neuroscience*, *3*(3), 201–215. <https://doi.org/10.1038/nrn755>

- De Schotten, M. T., Urbanski, M., Duffau, H., Volle, E., Lévy, R., Dubois, B., & Bartolomeo, P. (2005). Neuroscience: Direct evidence for a parietal-frontal pathway subserving spatial awareness in humans. *Science*, *309*(5744), 2226–2228. <https://doi.org/10.1126/science.1116251>
- Decety, J., & Lamm, C. (2007). The role of the right temporoparietal junction in social interaction: How low-level computational processes contribute to meta-cognition. *Neuroscientist*, *13*(6), 580–593. <https://doi.org/10.1177/1073858407304654>
- DiQuattro, N. E., & Geng, J. J. (2011). Contextual knowledge configures attentional control networks. *Journal of Neuroscience*, *31*(49), 18026–18035. <https://doi.org/10.1523/JNEUROSCI.4040-11.2011>
- Doesburg, S. M., Bedo, N., & Ward, L. M. (2016). Top-down alpha oscillatory network interactions during visuospatial attention orienting. *NeuroImage*, *132*, 512–519. <https://doi.org/10.1016/j.neuroimage.2016.02.076>
- Dombert, P. L., Kuhns, A., Mengotti, P., Fink, G. R., & Vossel, S. (2016). Functional mechanisms of probabilistic inference in feature- and space-based attentional systems. *NeuroImage*, *142*, 553–564. <https://doi.org/10.1016/j.neuroimage.2016.08.010>
- Donchin, E., & Coles, M. G. H. (1998). Context updating and the P300. *Behavioral and Brain Sciences*, *21*(1), 152–154. <https://doi.org/10.1017/s0140525x98230950>
- Doricchi, F., Lasaponara, S., Pazzaglia, M., & Silvetti, M. (2022). Left and right temporal-parietal junctions (TPJs) as “match/mismatch” hedonic machines: A unifying account of TPJ function. *Physics of Life Reviews*, *42*, 56–92. <https://doi.org/10.1016/j.plrev.2022.07.001>
- Doricchi, F., Macci, E., Silvetti, M., & Macaluso, E. (2010). Neural Correlates of the Spatial and Expectancy Components of Endogenous and Stimulus-Driven Orienting of Attention in the Posner Task. *Cerebral Cortex*, *20*(7), 1574–1585. <https://doi.org/10.1093/cercor/bhp215>
- Downar, J., Crawley, A. P., Mikulis, D. J., & Davis, K. D. (2001). The effect of task relevance on the cortical response to changes in visual and auditory stimuli: An event-related fMRI study. *NeuroImage*, *14*(6), 1256–1267.

<https://doi.org/10.1006/nimg.2001.0946>

- Dugué, L., Merriam, E. P., Heeger, D. J., & Carrasco, M. (2018). Specific visual subregions of TPJ mediate reorienting of spatial attention. *Cerebral Cortex*, 28(7), 2375–2390. <https://doi.org/10.1093/cercor/bhx140>
- Filipowicz, A., Valadao, D., Anderson, B., & Danckert, J. (2018). Rejecting Outliers: Surprising changes do not always improve belief updating. *Decision*, 5(3), 165–176. <https://doi.org/10.1037/dec0000073>
- Friston, K., & Kiebel, S. (2009). Predictive coding under the free-energy principle. *Philosophical Transactions of the Royal Society B: Biological Sciences*, 364(1521), 1211–1221. <https://doi.org/10.1098/rstb.2008.0300>
- Geng, J. J., & Vossel, S. (2013). Re-evaluating the role of TPJ in attentional control: Contextual updating? In *Neuroscience and Biobehavioral Reviews* (Vol. 37, Issue 10, pp. 2608–2620). Pergamon. <https://doi.org/10.1016/j.neubiorev.2013.08.010>
- Go, H., Danckert, J., & Anderson, B. (2022). Saccadic eye movement metrics reflect surprise and mental model updating. *Attention, Perception, and Psychophysics*, 84(5), 1553–1565. <https://doi.org/10.3758/s13414-022-02512-4>
- Gómez, C. M., Arjona, A., Donnarumma, F., Maisto, D., Rodríguez-Martínez, E. I., & Pezzulo, G. (2019). Tracking the time course of Bayesian inference with event-related potentials: A study using the central Cue Posner Paradigm. *Frontiers in Psychology*, 10(JUN), 1–14. <https://doi.org/10.3389/fpsyg.2019.01424>
- Gómez, C. M., Flores, A., Digiaco, M. R., & Vázquez-Marrufo, M. (2009). Sequential P3 effects in a Posner's spatial cueing paradigm: Trial-by-trial learning of the predictive value of the cue. *Acta Neurobiologiae Experimentalis*, 69(2), 155–167. <https://doi.org/10.55782/ane-2009-1741>
- Gratton, G. (2000). “Opt-cont” and “opt-3D”: A software suite for the analysis and 3D reconstruction of the event-related optical signal (EROS). *Psychophysiology*, 37.
- Gratton, G. (2010). Fast optical imaging of human brain function. *Frontiers in Human Neuroscience*, 4, 52. <https://doi.org/10.3389/fnhum.2010.00052>

- Gratton, G., Corballis, P. M., Cho, E., Fabiani, M., & Hood, D. C. (1995). Shades of gray matter: Noninvasive optical images of human brain responses during visual stimulation. *Psychophysiology*, *32*(5), 505–509.
<https://doi.org/10.1111/j.1469-8986.1995.tb02102.x>
- Gratton, G., & Fabiani, M. (2001). The event-related optical signal: A new tool for studying brain function. *International Journal of Psychophysiology*, *42*(2), 109–121. [https://doi.org/10.1016/S0167-8760\(01\)00161-1](https://doi.org/10.1016/S0167-8760(01)00161-1)
- Indovina, I., & MacAluso, E. (2007). Dissociation of stimulus relevance and saliency factors during shifts of visuospatial attention. *Cerebral Cortex*, *17*(7), 1701–1711. <https://doi.org/10.1093/cercor/bhl081>
- Käsbauer, A. S., Mengotti, P., Fink, G. R., & Vossel, S. (2020). Resting-state functional connectivity of the right temporoparietal junction relates to belief updating and reorienting during spatial attention. *Journal of Cognitive Neuroscience*, *32*(6), 1130–1141. https://doi.org/10.1162/jocn_a_01543
- Kelley, T. A., Serences, J. T., Giesbrecht, B., & Yantis, S. (2008). Cortical mechanisms for shifting and holding visuospatial attention. *Cerebral Cortex*, *18*(1), 114–125. <https://doi.org/10.1093/cercor/bhm036>
- Kiebel, S. J., Poline, J. B., Friston, K. J., Holmes, A. P., & Worsley, K. J. (1999). Robust smoothness estimation in statistical parametric maps using standardized residuals from the general linear model. *NeuroImage*, *10*(6), 756–766. <https://doi.org/10.1006/nimg.1999.0508>
- Krall, S. C., Rottschy, C., Oberwelland, E., Bzdok, D., Fox, P. T., Eickhoff, S. B., Fink, G. R., & Konrad, K. (2015). The role of the right temporoparietal junction in attention and social interaction as revealed by ALE meta-analysis. *Brain Structure and Function*, *220*(2), 587–604.
<https://doi.org/10.1007/s00429-014-0803-z>
- Lauritzen, T. Z., D’Esposito, M., Heeger, D. J., & Silver, M. A. (2009). Top-down flow of visual spatial attention signals from parietal to occipital cortex. *Journal of Vision*, *9*(13), 18–18. <https://doi.org/10.1167/9.13.18>
- Leitão, J., Thielscher, A., Tünerhoff, J., & Noppeney, U. (2015). Concurrent TMS-fMRI reveals interactions between dorsal and ventral attentional systems. *Journal of Neuroscience*, *35*(32), 11445–11457.

<https://doi.org/10.1523/JNEUROSCI.0939-15.2015>

- Luck, S. J. (1999). Direct and indirect integration of event-related potentials, functional magnetic resonance images, and single-unit recordings. *Human Brain Mapping*, 8(2–3), 115–120. [https://doi.org/10.1002/\(SICI\)1097-0193\(1999\)8:2/3<115::AID-HBM8>3.0.CO;2-3](https://doi.org/10.1002/(SICI)1097-0193(1999)8:2/3<115::AID-HBM8>3.0.CO;2-3)
- Mengotti, P., Dombert, P. L., Fink, G. R., & Vossel, S. (2017). Disruption of the right temporoparietal junction impairs probabilistic belief updating. *Journal of Neuroscience*, 37(22), 5419–5428. <https://doi.org/10.1523/JNEUROSCI.3683-16.2017>
- Mengotti, P., Käsbaier, A. S., Fink, G. R., & Vossel, S. (2020). Lateralization, functional specialization, and dysfunction of attentional networks. *Cortex*, 132, 206–222. <https://doi.org/10.1016/j.cortex.2020.08.022>
- Mort, D. J., Malhotra, P., Mannan, S. K., Rorden, C., Pambakian, A., Kennard, C., & Husain, M. (2003). The anatomy of visual neglect. *Brain*, 126(9), 1986–1997. <https://doi.org/10.1093/brain/awg200>
- Natale, E., Marzi, C. A., & Macaluso, E. (2009). fMRI correlates of visuo-spatial reorienting investigated with an attention shifting double-cue paradigm. *Human Brain Mapping*, 30(8), 2367–2381. <https://doi.org/10.1002/hbm.20675>
- Natale, E., Marzi, C. A., & Macaluso, E. (2010). Right temporal-parietal junction engagement during spatial reorienting does not depend on strategic attention control. *Neuropsychologia*, 48(4), 1160–1164. <https://doi.org/10.1016/j.neuropsychologia.2009.11.012>
- O'Reilly, J. X., Schüffelgen, U., Cuell, S. F., Behrens, T. E. J., Mars, R. B., & Rushworth, M. F. S. (2013). Dissociable effects of surprise and model update in parietal and anterior cingulate cortex. *Proceedings of the National Academy of Sciences of the United States of America*, 110(38). <https://doi.org/10.1073/pnas.1305373110>
- Oldfield, R. C. (1971). The assessment and analysis of handedness: The Edinburgh inventory. *Neuropsychologia*, 9(1), 97–113. [https://doi.org/10.1016/0028-3932\(71\)90067-4](https://doi.org/10.1016/0028-3932(71)90067-4)
- Parisi, G., Mazzi, C., Colombari, E., Chiarelli, A. M., Metzger, B. A., Marzi, C.

- A., & Savazzi, S. (2020). Spatiotemporal dynamics of attentional orienting and reorienting revealed by fast optical imaging in occipital and parietal cortices. *NeuroImage*, 222(April), 117244.
<https://doi.org/10.1016/j.neuroimage.2020.117244>
- Polich, J. (2007). Updating P300: An integrative theory of P3a and P3b. In *Clinical Neurophysiology* (Vol. 118, Issue 10, pp. 2128–2148). Elsevier.
<https://doi.org/10.1016/j.clinph.2007.04.019>
- Posner, M. I. (1980). Orienting of attention. *Quarterly Journal of Experimental Psychology*, 32(1), 3–25. <https://doi.org/10.1080/00335558008248231>
- Posner, M. I., Walker, J. A., Friedrich, F. J., & Rafal, R. D. (1984). Effects of Parietal Attention ' Injury on Covert of. *The Journal of Neuroscience : The Official Journal of the Society for Neuroscience*, 4(7), 1863–1874.
- Proskovec, A. L., Heinrichs-Graham, E., Wiesman, A. I., McDermott, T. J., & Wilson, T. W. (2018). Oscillatory dynamics in the dorsal and ventral attention networks during the reorienting of attention. *Human Brain Mapping*, 39(5), 2177–2190. <https://doi.org/10.1002/hbm.23997>
- Ptak, R., & Schnider, A. (2010). The dorsal attention network mediates orienting toward behaviorally relevant stimuli in spatial neglect. *Journal of Neuroscience*, 30(38), 12557–12565.
<https://doi.org/10.1523/JNEUROSCI.2722-10.2010>
- Rihs, T. A., Michel, C. M., & Thut, G. (2009). A bias for posterior α -band power suppression versus enhancement during shifting versus maintenance of spatial attention. *NeuroImage*, 44(1), 190–199.
<https://doi.org/10.1016/j.neuroimage.2008.08.022>
- Rizzolatti, G., Riggio, L., Dascola, I., & Umiltá, C. (1987). Reorienting attention across the horizontal and vertical meridians: Evidence in favor of a premotor theory of attention. *Neuropsychologia*, 25(1 PART 1), 31–40.
[https://doi.org/10.1016/0028-3932\(87\)90041-8](https://doi.org/10.1016/0028-3932(87)90041-8)
- Rossi, S., Hallett, M., Rossini, P. M., Pascual-Leone, A., Avanzini, G., Bestmann, S., Berardelli, A., Brewer, C., Canli, T., Cantello, R., Chen, R., Classen, J., Demitrack, M., Di Lazzaro, V., Epstein, C. M., George, M. S., Fregni, F., Ilmoniemi, R., Jalinous, R., ... Ziemann, U. (2009). Safety, ethical

- considerations, and application guidelines for the use of transcranial magnetic stimulation in clinical practice and research. *Clinical Neurophysiology*, *120*(12), 2008–2039.
<https://doi.org/10.1016/j.clinph.2009.08.016>
- Scholz, J., Triantafyllou, C., Whitfield-Gabrieli, S., Brown, E. N., & Saxe, R. (2009). Distinct regions of right temporo-parietal junction are selective for theory of mind and exogenous attention. *PLoS ONE*, *4*(3).
<https://doi.org/10.1371/journal.pone.0004869>
- Schuwerk, T., Grosso, S. S., & Taylor, P. C. J. (2021). The influence of TMS of the rTPJ on attentional control and mentalizing. *Neuropsychologia*, *162*(October), 108054.
<https://doi.org/10.1016/j.neuropsychologia.2021.108054>
- Schuwerk, T., Schurz, M., Müller, F., Rupprecht, R., & Sommer, M. (2017). The rTPJ's overarching cognitive function in networks for attention and theory of mind. *Social Cognitive and Affective Neuroscience*, *12*(1), 157–168.
<https://doi.org/10.1093/scan/nsw163>
- Simpson, G. V., Weber, D. L., Dale, C. L., Pantazis, D., Bressler, S. L., Leahy, R. M., & Luks, T. L. (2011). Dynamic activation of frontal, parietal, and sensory regions underlying anticipatory visual spatial attention. *Journal of Neuroscience*, *31*(39), 13880–13889.
<https://doi.org/10.1523/JNEUROSCI.1519-10.2011>
- Spadone, S., Wyczesany, M., Della Penna, S., Corbetta, M., & Capotosto, P. (2021). Directed Flow of Beta Band Communication during Reorienting of Attention within the Dorsal Attention Network. *Brain Connectivity*, *11*(9), 717–724. <https://doi.org/10.1089/brain.2020.0885>
- Vandenberghe, R., Molenberghs, P., & Gillebert, C. R. (2012). Spatial attention deficits in humans: The critical role of superior compared to inferior parietal lesions. *Neuropsychologia*, *50*(6), 1092–1103.
<https://doi.org/10.1016/j.neuropsychologia.2011.12.016>
- Vossel, S., Geng, J. J., & Fink, G. R. (2014). Dorsal and ventral attention systems: distinct neural circuits but collaborative roles. *The Neuroscientist : A Review Journal Bringing Neurobiology, Neurology and Psychiatry*, *20*(2), 150–159.

<https://doi.org/10.1177/1073858413494269>

Vossel, S., Mathys, C., Daunizeau, J., Bauer, M., Driver, J., Friston, K. J., & Stephan, K. E. (2014). Spatial attention, precision, and bayesian inference: A study of saccadic response speed. *Cerebral Cortex*, *24*(6), 1436–1450.

<https://doi.org/10.1093/cercor/bhs418>

Vossel, S., Mathys, C., Stephan, K. E., & Friston, K. J. (2015). Cortical coupling reflects Bayesian belief updating in the deployment of spatial attention.

Journal of Neuroscience, *35*(33), 11532–11542.

<https://doi.org/10.1523/JNEUROSCI.1382-15.2015>

Vossel, S., Thiel, C. M., & Fink, G. R. (2006). Cue validity modulates the neural correlates of covert endogenous orienting of attention in parietal and frontal cortex. *NeuroImage*, *32*(3), 1257–1264.

<https://doi.org/10.1016/j.neuroimage.2006.05.019>

Vossel, S., Weidner, R., Driver, J., Friston, K. J., & Fink, G. R. (2012).

Deconstructing the architecture of dorsal and ventral attention systems with dynamic causal modeling. *Journal of Neuroscience*, *32*(31), 10637–10648.

<https://doi.org/10.1523/JNEUROSCI.0414-12.2012>

Vossel, S., Weidner, R., Thiel, C. M., & Fink, G. R. (2009). What is “Odd” in Posner’s Location-cueing Paradigm? Neural Responses to Unexpected Location and Feature Changes Compared. *Journal of Cognitive Neuroscience*, *21*(1), 30–41.

<https://doi.org/10.1162/jocn.2009.21003>

Wen, X., Yao, L., Liu, Y., & Ding, M. (2012). Causal interactions in attention networks predict behavioral performance. *Journal of Neuroscience*, *32*(4), 1284–1292.

<https://doi.org/10.1523/JNEUROSCI.2817-11.2012>

Whalen, C., Maclin, E. L., Fabiani, M., & Gratton, G. (2008). Validation of a method for coregistering scalp recording locations with 3D structural MR images. *Human Brain Mapping*, *29*(11), 1288–1301.

<https://doi.org/10.1002/hbm.20465>

Wisniewski, D., Reverberi, C., Momennejad, I., Kahnt, T., & Haynes, J. D. (2015). The role of the parietal cortex in the representation of task–reward associations. *Journal of Neuroscience*, *35*(36), 12355–12365.

<https://doi.org/10.1523/JNEUROSCI.4882-14.2015>

- Wolf, U., Wolf, M., Toronov, V., Michalos, A., Paunescu, L. A., & Gratton, E. (2014). Detecting cerebral functional slow and fast signals by frequency-domain near-infrared spectroscopy using two different sensors. *Biomedical Optical Spectroscopy and Diagnostics (2000)*, Paper TuF10, TuF10. <https://doi.org/10.1364/bosd.2000.tuf10>
- Worsley, K. J., Poline, J. B., Vandal, A. C., & Friston, K. J. (1995). Tests for distributed, nonfocal brain activations. *NeuroImage*, 2(3), 183–194. <https://doi.org/10.1006/nimg.1995.1024>